# *S*-Bacillithiolation Protects Against Hypochlorite Stress in *Bacillus subtilis* as Revealed by Transcriptomics and Redox Proteomics*[S]

**Bui Khanh Chi‡, Katrin Gronau‡, Ulrike Mäder§, Bernd Hessling‡, Dörte Becher‡, and Haike Antelmann‡¶**

**Protein *S*-thiolation is a post-translational thiol-modification that controls redox-sensing transcription factors and protects active site cysteine residues against irreversible oxidation. In *Bacillus subtilis* the MarR-type repressor OhrR was shown to sense organic hydroperoxides via formation of mixed disulfides with the redox buffer bacillithiol (Cys-GlcN-Malate, BSH), termed as *S*-bacillithiolation. Here we have studied changes in the transcriptome and redox proteome caused by the strong oxidant hypochloric acid in *B. subtilis.* The expression profile of NaOCl stress is indicative of disulfide stress as shown by the induction of the thiol- and oxidative stress-specific Spx, CtsR, and PerR regulons. Thiol redox proteomics identified only few cytoplasmic proteins with reversible thiol-oxidations in response to NaOCl stress that include GapA and MetE. Shotgun-liquid chromatography-tandem MS analyses revealed that GapA, Spx, and PerR are oxidized to intramolecular disulfides by NaOCl stress. Furthermore, we identified six *S*-bacillithiolated proteins in NaOCl-treated cells, including the OhrR repressor, two methionine synthases MetE and YxjG, the inorganic pyrophosphatase PpaC, the 3-D-phosphoglycerate dehydrogenase SerA, and the putative bacilliredoxin YphP. *S*-bacillithiolation of the OhrR repressor leads to upregulation of the OhrA peroxiredoxin that confers together with BSH specific protection against NaOCl. S-bacillithiolation of MetE, YxjG, PpaC and SerA causes hypochlorite-induced methionine starvation as supported by the induction of the S-box regulon. The mechanism of *S*-glutathionylation of MetE has been described in *Escherichia coli* also leading to enzyme inactivation and methionine auxotrophy. In summary, our studies discover an important role of the bacillithiol redox buffer in protection against hypochloric acid by *S*-bacillithiolation of the redox-sensing regulator OhrR and of four enzymes of the methionine biosynthesis pathway.**

From the ‡Institute for Microbiology and §Interfaculty Institute for Genetics and Functional Genomics, Ernst-Moritz-Arndt-University of Greifswald, D-17487 Greifswald, Germany

Received March 10, 2011, and in revised form, July 2, 2011
Published, MCP Papers in Press, July 12, 2011, DOI 10.1074/mcp.M111.009506

***Molecular & Cellular Proteomics 10: 10.1074/mcp.M111.009506, 1–21, 2011.***

Reactive oxygen species (ROS)[1] are an unavoidable consequence of the aerobic lifestyle of many organisms (1, 2). ROS can be generated by incomplete reduction of molecular oxygen during the respiratory chain. Pathogenic bacteria encounter ROS, such as hydrogen peroxide ($H_2O_2$), superoxide anion and hypochloric acid as defense of the innate immune response during host-pathogen interactions. Upon bacterial infection, myeloperoxidase is released from activated macrophages to produce the strong oxidant hypochloric acid from $H_2O_2$ and $Cl^-$ (3, 4).

ROS can damage all cellular macromolecules, such as proteins, lipids, carbohydrates, and nucleotides (2, 5). Cells activate the expression of antioxidant mechanisms to detoxify ROS and to repair the damage. The response of bacteria to $H_2O_2$ and organic hydroperoxides (ROOH) involves heme-cofactor containing catalases and thiol-dependent peroxidases as detoxification mechanisms (5, 6). Peroxidases use conserved redox-active cysteine residues that function in reduction of peroxides. These oxidative stress defense mechanisms are often controlled by redox-sensitive transcription factors that undergo post-translational thiol-modifications upon challenge with ROS leading either to activation or inactivation of the transcription factors (7). Post-translational thiol-modifications implicated in redox-sensing mechanisms are

[1] The abbreviations used are: ROS, reactive oxygen species; BSH, bacillithiol; Brx, bacilliredoxin; CHP, cumene hydroperoxide; Cys, cysteine; GlcNAc, N-acetyl glucoseamine; GSH, glutathione; GST, glutathione S-transferase; IAM, iodoacetamide; IP, immunoprecipitation; LMW, low molecular weight; Mal, malate; MSH, mycothiol; Met, methionine; MG, methylglyoxal; MHQ, methylhydroquinone; N5-THF, 5-methyltetrahydrofolate; N5,N10-THF, 5,10-methylenetetrahydrofolate; *PAPS, 3′-phosphoadenosine-5′-phosphosulfate*; $PP_i$, inorganic pyrophosphate; ROOH, organic hydroperoxide; ROH, organic alcohol; RES, reactive electrophilic species; RuMP, ribulose-5-monophosphate; THF, tetrahydrofolate; TrxAB, thioredoxin/thioredoxin reductase; RNS, reactive nitrogen species; FOX, ferrous oxidation xylenol orange.

known as thiol-disulfide redox-switches and include in most cases inter- or intramolecular disulfides and mixed disulfides with low molecular weight (LMW) thiols (*S*-thiolations). The best studied examples for peroxide-sensing thiol-based transcription factors are *Escherichia coli* OxyR (8–11) and yeast Yap1 transcription factor (7, 12, 13) that are activated by intramolecular disulfide bond formation to induce the antioxidant defense mechanisms.

In *Bacillus subtilis*, the major detoxification enzymes for peroxides are catalase (KatA) and alkylhydroperoxide reductase (AhpCF) that are controlled of the peroxide-sensing Fur family metalloregulatory PerR repressor (5). PerR harbors a structural Zn-binding site coordinated by four cysteine residues and a regulatory Fe or Mn binding site consisting of His and Asp residues. Inactivation of PerR is caused by Fe-catalyzed oxidation of His37 and His91 to 2-oxohistidine in the regulatory site (5, 14–16). The response to ROOH involves the MarR-type repressor OhrR in *B. subtilis* that is conserved in many other bacteria (6, 7). OhrR-like proteins control a thiol-dependent peroxiredoxin that converts ROOH to organic alcohols. OhrR proteins can be devided into the one and two-Cys families of redox sensing repressors. The OhrR protein of *Xanthomonas campestris* belongs to the two-Cys family that is oxidized to a Cys22-Cys127' intermolecular disulfide between both subunits of the OhrR dimer (17). One-Cys OhrR proteins harbor one conserved N-terminal Cys with the prototype of *B. subtilis* OhrR or *Staphylococcus aureus* SarZ and MgrA (7, 18). Cumene hydroperoxide (CHP) leads to Cys15 oxidation to sulfenic acid that is rapidly oxidized to *S*-thiolated OhrR containing cysteine or the redox buffer bacillithiol (BSH) (19, 20). Thus, *B. subtilis* OhrR is controlled by *S*-cysteinylation and *S*-bacillithiolation as redox-switch mechanism leading to inactivation of the OhrR repressor function and derepression of *ohrA* transcription.

In previous studies, we investigated the global response, post-translational modifications and specific regulatory mechanisms that are induced by reactive electrophilic species (RES) in *B. subtilis,* such as diamide, quinones, or aldehydes. RES deplete the cellular redox buffer cysteine leading to induction of the Spx-regulon that controls thiol-disulfide oxidoreductases (TrxAB) to restore the redox homeostasis (21–23). *B. subtilis* encodes specific redox-sensing regulators of the MarR/DUF24-family that sense RES, but not ROS (7). These include the paralogous repressors YodB and CatR that are inactivated via intermolecular disulfide formation by diamide and quinones resulting in derepression of the azoreductase (AzoR1), nitroreductase (YodC), and thiol-dependent dioxygenase (CatE) catalyzing the detoxification of the electrophiles (24–26). Other proteins of the MarR/DUF24-family (HxlR) and of the MerR/NmlR-family (AdhR) sense specifically aldehydes, such as formaldehyde and methylglyoxal (23).

In this study, we were interested in the global response, regulatory mechanisms, and post-translational thiol-modifications that contribute to the resistance of *B. subtilis* to the strong oxidant hypochloric acid. Hypochloric acid is the active component of household bleach and widely used as antimicrobial disinfectant to clean surfaces. The bactericidal effect of hypochloric acid has been proposed to involve generation of ROS, such as superoxide anion and hydroxyl radical formation in *E. coli* (27). Recent redox proteomics studies in *E. coli* using the OxICAT approach have shown that bleach causes strong disulfide formation and protein aggregation in a different set of proteins than $H_2O_2$ (28). As defense mechanism against NaOCl stress, *E. coli* uses the redox controlled chaperone Hsp33 that is activated by NaOCl by the formation of intramolecular disulfides in the Zn-redox switch centers resulting in Zn release, oxidative unfolding and dimerization (29). Hsp33 protects cells against NaOCl-induced protein aggregation. The mode of action has been also studied using transcriptome analyses in pathogenic *E. coli* O157:H7 outbreak strains and the food-borne pathogen *B. cereus* ATCC14579 (30, 31). Both transcriptome analyses suggest a major oxidative stress response mechanism of NaOCl. Regulons involved in the biosynthesis of sulfur and sulfur-containing amino acids were up-regulated by NaOCl in both genome-wide studies. However, the mode of action of hypochloric acid has not yet been investigated in *B. subtilis*.

We have used transcriptomic and redox proteomic approaches coupled with shotgun-LC-MS/MS analyses to analyze the mode of action and reversible thiol-modifications by NaOCl stress in *B. subtilis*. We discovered that the major resistant determinant to NaOCl is the OhrA peroxiredoxin that conferred specific protection against NaOCl toxicity. Moreover, we identified *S*-bacillithiolations of the OhrR repressor, two methionine synthases MetE and YxjG, the inorganic pyrophosphatase PpaC, and the 3-D-phosphoglycerate dehydrogenase SerA as major protection mechanisms against hypochlorite stress in *B. subtilis*.

## EXPERIMENTAL PROCEDURES

*Bacterial Strains and Growth Conditions*—The bacterial strains used were *B. subtilis* wild-type strains 168 (*trpC2*), JH642 (*trpC2* attSP$\beta$), and CU1065 (*trpC2* pheA1) and mutant strains Δ*spx* (*trpC2*,*spx*::*neo*$^r$) (32), Δ*ohrR* (*trpC2*,*ohrR*::*cm*$^r$), Δ*ohrA* (*trpC2*, *ohrA*::cm$^r$), Δ*sigB* (*trpC2*,*sigB*::*cm*$^r$), Δ*perR* (*trpC2*,*perR*::*cm*$^r$) (33), HB9121 (CU1065 *trpC2*,*ohrR*::km$^r$ *ohrR*-FLAG (Spc$^r$) *ohrA-cat lacZ* (Neo$^r$) (19), HB2048 (CU1065 SP$\beta$*c2*Δ*2*::Tn*917*::(*ohrA-cat-lacZ*)*ohrR::kan*,*thrC::pXTohrRC15S*) (34), HB11002 (CU1065 *trpC2*, *bshA*::mls$^r$), and HB11053 (CU1065 *trpC2*, *bshB1*:: *spc*$^r$ *bshB2::cm*$^r$) (35). *B. subtilis* strains were cultivated under vigorous agitation at 37 °C in Belitsky minimal medium (BMM) as described previously (36). The antibiotics were used at the following concentrations: 1 $\mu$g/ml erythromycin, 25 $\mu$g/ml lincomycin, 5 $\mu$g/ml chloramphenicol, 10 $\mu$g/ml kanamycin, and 100 $\mu$g/ml spectinomycin. Sodium hypochlorite (15% stock solution), diamide, and cumene hydroperoxide were purchased from Sigma Aldrich.

For NaOCl stress exposure, cells were grown in BMM to an optical density at 500 nm ($OD_{500}$) of 0.4 and treated with 50, 75, or 100 $\mu$M NaOCl diluted freshly in destilled water. The growth experiments in the presence of methionine were performed by addition of 75 $\mu$M

methionine either after inoculation of the culture or 30 and 60 min after NaOCl stress exposure.

Gene deletions for construction of the *ohrA* mutant were generated using long-flanking-homology polymerase chain reaction (LFH-PCR) as described previously (25). Primers ohrA-F1 (5′-TGCAGCTGATTGAGGATACG-3′) and ohrA-F2 (5′-GTTATCCGCTCACAATTCGCGGTCTGATGAAATGACCT-3′) were used to amplify the up fragment and primers ohrA-R1 (5′-CGTCGTGACTGGGAAAACGGTGTGACGCTGCAAGTAAA-5′) and ohrA-R2 (5′-CCCTTCAATCTCCGAATCAA-3′) to amplify the down fragment, respectively. Fragments were amplified and joined together with the chloramphenicol cassette using *Pfusion* DNA polymerase (Invitrogen, Carlsbad, CA) as described (33). Integration and deletion of the *ohrA* gene were confirmed by PCR and by Northern blot analysis using digoxigenin-labeled RNA probes of the corresponding gene.

*Analysis of NaOCl Concentrations in the Cell Culture Supernatant Using the FOX Assay*—The concentrations of the remaining NaOCl in the culture supernatants were determined using the FOX assay (37). FOX reagent was prepared by mixing 100 ml FOX I (100 mM sorbitol, 125 μM xylenol orange) and 1 ml FOX II (25 mM ammonious ferrous-(II)sulfate in 2.5 M $H_2SO_4$). It was not possible to measure any NaOCl concentrations in BMM with tryptophane and glutamate. Thus, cells were grown to an $OD_{500}$ of 0.4 in BMM, centrifuged and resuspended in BMM without tryptophane and glutamate before the addition of 75 μM NaOCl. Samples of 500 μl medium were taken at different time points after NaOCl addition, mixed with 500 μl FOX reagent and incubated at room temperature for 60 min. The absorbance was measured at 560 nm. Calibration curves were generated using NaOCl concentrations in the range from 0 to 100 μM diluted in BMM without tryptophane and glutamate.

*Thiol Redox Proteome Analysis*—The thiol redox proteome analysis was performed as described previously (38) with the modifications as explained (21). Cells were harvested before (control conditions) and 10, 20, and 30 min after exposure to 50 μM NaOCl stress, resuspended in urea/CHAPS alkylation buffer (8 M urea; 1% CHAPS; 1 mM EDTA; 200 mM Tris-HCl pH 8,0; 100 mM iodoacetamide (IAM)), sonicated, alkylated for 20 min in the dark, precipitated with 100% acetone, washed several times with 80% acetone and dried. After resolving in urea/CHAPS buffer without IAM, 200 μg of the protein extract were reduced with 10 mM Tris-(2-carboxyethyl)-phosphine (TCEP) and labeled with BODIPY FL $C_1$-IA [*N*-(4,4-difluoro-5,7-dimethyl-4-bora-3a,4a-diaza-*s*-indacene-3-yl)-methyl)-iodoacetamide] (Invitrogen, Eugene, OR). The fluorescence-labeled protein extract was separated using 2D PAGE as described (21). The two-dimensional (2D) gels were scanned using a Typhoon 9400 variable mode imager (Amersham Biosciences, Freiburg, Germany) for BODIPY-fluorescence and then stained with Colloidal Coomassie for protein amounts. Quantitative image analysis was performed with the DECODON Delta 2D software (http://www.decodon.com).

The first alkylation protocol (38) that applied the TCA-precipitation step to harvest cells to stop thiol-disulfide exchanges was changed previously (21) for two reasons: (1) The 2D gels were of bad quality and exhibited protein streaking during the isoelectric focusing (IEF) and (2) GapA was oxidized artificially by this TCA precipitation step under control conditions but not if this TCA step was omitted (38) and GapA is an important redox-controlled cytoplasmic marker protein and strongly oxidized in response to quinones and diamide (21, 22). Because GapA was neither oxidized using our alkylation protocol in the redox proteome of control cells nor in the LC-MS/MS approach, this indicates no artificial thiol-disulfide exchange during our sample preparations.

*Identification of Reversibly Oxidized Proteins in the Thiol-Redox Proteome Using Matrix-Assisted Laser Desorption Ionization/Time Of Flight-TOF Tandem MS (MS/MS)*—Tryptic digestion of the reversibly oxidized proteins in the Coomassie-stained thiol-redox proteome was performed manually as described previously (24). In brief, gel pieces were washed 3–5 times with 1 ml of 20 mM (w/v) ammonium bicarbonate, pH 8.0/50% (v/v) acetonitrile (ACN) for 30 min and once with 1 ml 75% ACN for 30 min. Gel pieces were dried and the proteins in-gel digested with 20 μg/μl trypsin dissolved in water (Promega, Madison, WI) at 37 °C for 16 h. Tryptic peptides were eluted with 0.5% (w/v) trifluoroacetic acid/50% (v/v) ACN and 0.5 μl of this peptide solution was spotted on the MALDI-targets. Then, 0.5 μl of matrix solution (50% (v/v) ACN/0.5% (w/v) trifluoroacetic acid) saturated with α-cyano-4-hydroxy cinnamic acid was mixed with the spotted tryptic peptides and dried on the target for 15 min.

The matrix-assisted laser desorption ionization/time of flight (MALDI-TOF)-TOF measurement of spotted peptide solutions was carried out on a Proteome-Analyzer 4800 (Applied Biosystems, Foster City, CA). The spectra were recorded in reflector mode in a mass range from 900 to 3700 Da with a focus mass of 2000 Da. For one main spectrum 25 subspectra with 100 shots per subspectrum were accumulated using a random search pattern. If the autolytical fragment of trypsin with the monoisotopic $(M+H)^+$ *m/z* at 2211.104 reached a signal to noise ratio (S/N) of at least 10, an internal calibration was automatically performed using this peak for one-point-calibration. The peptide search tolerance was 50 ppm but the actual RMS value was between 10 and 20 ppm. After calibration the peak lists were created by using the "peak to mascot" script of the GPS Explorer™ software version 3.6 with the following settings: mass range from 900 to 3700 Da; peak density of 50 peaks per range of 200 Da; minimal area of 100 and maximal 200 peaks per protein spot and minimal S/N ratio of 6. The peak lists were searched against a *Bacillus subtilis* sequence database extracted from UniprotKB release 12.7 (UniProt Consortium, Nucleic acids research 2007, 35, D193–197) using the Mascot search engine version 2.1.04 (Matrix Science Ltd, London, UK).

MALDI-TOF-TOF MS/MS analysis was performed for the three strongest peaks of the TOF-spectrum. For one main spectrum 20 sub-spectra with 125 shots per subspectrum were accumulated using a random search pattern. The internal calibration was automatically performed as one-point-calibration if the mono-isotopic arginine $(M+H)^+$ *m/z* at 175.119 or lysine $(M+H)^+$ *m/z* at 147.107 reached a S/N of at least 5. The peak lists were created by using the "peak to mascot" script of the GPS Explorer™ software version 3.6 with the following settings: mass range from 60 Da to a mass that was 20 Da lower than the precursor mass; peak density of 5 peaks per 200 Da; minimal area of 100 and maximal 20 peaks per precursor and a minimal S/N ratio of 5. Peptide mixtures that yielded a mowse score of at least 50 in the reflector mode and a sequence coverage of at least 30% that were confirmed by subsequent MS/MS analysis were regarded as positive identification. The complete Mascot search results including the MS and MS/MS data of all protein identifications are shown in supplemental Figs. S1*A–P*.

*Immunoprecipitation (IP) and Nonreducing SDS-PAGE Analysis of the OhrR-FLAG Protein*—The OhrR-FLAG protein expressing *B. subtilis* strain HB9121 was grown in BMM and treated with 50 μM NaOCl at an $OD_{500}$ of 0.4. Cells were harvested before (control conditions) and 15 min after NaOCl-treatment in TE-buffer (10 mM Tris-HCl, pH8; 1 mM EDTA) with 100 mM IAM. Cells were sonicated, the protein extracts obtained after repeated centrifugation and alkylated in the dark for 20 min. OhrR-FLAG protein was purified by IP using anti-FLAG M2-affinity agarose (Invitrogen) according to the instructions of the manufacturer. The precipitated OhrR-FLAG protein was eluted by boiling in non-reducing SDS sample buffer (4% SDS; 62.5 mM Tris-HCl pH 8.0, glycerol) and separated using 15% nonreducing SDS-PAGE. The OhrR-FLAG protein band of the expected size was cut

from the SDS-gel, tryptically digested as described above and analyzed by LTQ-Orbitrap mass spectrometry.

*LTQ-Orbitrap Velos Mass Spectrometry and Identification of Post-translational Thiol-modifications*—*B. subtilis* wild-type and Δ*bshA* mutant cells were harvested before (control conditions) and 15 min after exposure to 50 μM NaOCl stress. Cells were resuspended in urea/CHAPS alkylation buffer with 100 mM IAM as described above and sonicated to obtain the alkylated protein extracts. The alkylated protein extracts were separated using 15% nonreducing SDS-PAGE (200 μg each per lane) and the complete lanes were cut into 10 gel pieces and digested with trypsin as described above. Peptides eluted from tryptic digests of gel pieces were subjected to a reversed phase column chromatography (self packed C18 column, 100-μm i. D. x 200 mm) operated on a Easy-nLC II (Thermo Fisher Scientific, Waltham, MA). Elution was performed by a binary gradient of buffer A (0.1% (v/v) acetic acid) and B (99.9% (v/v) ACN, 0.1% (v/v) acetic acid) over a period of 100 min with a flow rate of 300 nl/min. MS and MS/MS data were acquired with the LTQ-Orbitrap-Velos mass spectrometer (Thermo Fisher Scientific) equipped with a nanoelectrospray ion source. The Orbitrap Velos was operated in data-dependent MS/MS mode using the lock-mass option for real time recalibration. After a survey scan in the Orbitrap ($r$ = 30,000) MS/MS data were recorded for the 20 most intensive precursor ions in the linear ion trap. Singly charged ions were not taken into account for MS/MS analysis.

Post-translational modifications of proteins were identified by searching all MS/MS spectra in "dta" format against an *B. subtilis* target-decoy protein sequence database (8294 entries) using Sorcerer™-SEQUEST® (Sequest version 2.7 rev. 11, Thermo Electron including Scaffold_3_00_02, Proteome Software Inc., Portland, OR). The target-decoy database includes the complete proteome set of *B. subtilis* 168 (4105 database entries) that was extracted from UniprotKB release 12.7 (UniProt Consortium, Nucleic acids research 2007, 35, D193–197) (39) and an appended set of 4147 reversed sequences and 42 sequences of common laboratory contaminants created by BioworksBrowser version 3.2 (Thermo Electron Corp.) according to Elias *et al.* (40). The Sequest search was carried out considering the following parameter: a parent ion mass tolerance 10 ppm, fragment ion mass tolerance of 1.00 Da. Up to two tryptic miscleavages were allowed. Methionine oxidation (+15.994915 Da) and cysteine carbamidomethylation (+57.021464 Da) were set as variable modifications. Multiple Sequest searches were performed for either intramolecular disulfide bonds (−2.01565 Da), *S*-cysteinylations (+119.004099 Da for $C_3H_7NO_2S$) or *S*-bacillithiolations (+396.083866 Da for $C_{13}H_{22}N_2O_{10}S$) as variable post-translational cysteine modifications, allowing a maximum of three modifications per peptide in each Sequest search.

Proteins were identified by at least two peptides applying a stringent SEQUEST filter. Sequest identifications required at least ΔCn scores of greater than 0.10 and XCorr scores of greater than 1.9, 2.2, 3.3, and 3.75 for singly, doubly, triply and quadruply charged peptides. The complete CID MS/MS spectra of the modified Cys-containing peptides and the corresponding b and y fragment ion series are given in detail in supplemental Figs. S2 and S3. The Sequest search results are submitted as "dta" and "out" files to the PRIDE database (http://www.ebi.ac.uk/pride/) (41) and deposited under the accession numbers 17516–17659.

*Transcriptome Analysis*—For microarray analysis, *B. subtilis* wild-type cells were grown in minimal medium to $OD_{500}$ of 0.4 and harvested before and 10 min after exposure to 50 μM NaOCl. Total RNA was isolated by the acid phenol method as described (42). For transcriptome analysis, 35 μg RNA were DNase-treated using the RNase-Free DNase Set (Qiagen) and purified using the RNA Clean-Up and Concentration Micro Kit (Norgen). The quality of the RNA preparations was assessed by means of the Agilent 2100 Bioanalyzer according to the manufacturer's instructions. Synthesis and purification of fluorescently labeled cDNA were carried out as descibed (43) with minor modifications. In detail, 10 μg of total RNA were mixed with random primers (Promega) and spike-ins (Two-Color RNA Spike-In Kit, Agilent Technologies, Santa Clara, CA). The RNA/primer mixture was incubated at 70 °C for 10 min followed by 5 min incubation on ice. Then, the following reagents were added: 10 μl of 5x First Strand Buffer (Invitrogen), 5 μl of 0.1 M DTT (Invitrogen), 0.5 μl of a dNTP mix (10 mM dATP, dGTP, and dTTP, 2.5 mM dCTP), 1.25 μl of Cy3-dCTP or Cy5-dCTP (GE Healthcare) and 2 μl of SuperScript II reverse transcriptase (Invitrogen). The reaction mixture was incubated at 42 °C for 60 min and then heated to 70 °C for 10 min. After 5 min on ice, the RNA was degraded by incubation with 2 units of RNaseH (Invitrogen) at room temperature for 30 min. Labeled cDNA was then purified using the CyScribe GFX Purification Kit (GE Healthcare). The individual samples were labeled with Cy5, whereas the reference pool was labeled with Cy3. 500 ng of Cy5-labeled cDNA and 500 ng of Cy3-labeled cDNA were hybridized together to the microarray following Agilent's hybridization, washing and scanning protocol (Two-Color Microarray-based Gene Expression Analysis, version 5.5). Data were extracted and processed using the Feature Extraction software (version 10.5, Agilent Technologies). For each gene on a microarray, the error-weighted average of the log ratio values of the individual probes was calculated using the Rosetta Resolver software (version 7.2.1, Rosetta Biosoftware). Genes showing induction or repression ratios of at least threefold in three independent experiments were considered as significantly induced. The averages ratios and standard deviations for all induced or repressed genes are calculated from three independent transcriptome experiments after 10 min of exposure to NaOCl stress and listed in supplemental Table S1 and S2. All microarray datasets are available in the GEO database under accession numbers [GSE27637].

*Hierarchical Clustering Analysis*—Clustering of gene expression profiles was performed using Cluster 3.0 (44). The transcriptome data sets were derived from previous publications and this study and included log2-fold expression changes 10 min after exposure of *B. subtilis* to diamide (1 mM) (45), methylhydroquinone (MHQ) (0.33 mM) (46), catechol (2.4 mM) (47), formaldehyde (1 mM), methylglyoxal (MG) (2.8 and 5.6 mM) (23), and 50 μM NaOCl. After hierarchical clustering, the output was visualized using TreeView (48). For the clustering 630 genes were selected that are induced by RES and NaOCl stress in *B. subtilis* (*e.g.* CtsR, CymR, Spx, PerR, ArsR, CsoR, CzrA, OhrR, YodB, YvaP (CatR), MhqR, LexA, SigmaD, AdhR, and HxlR regulons) (supplemental Table S4).

*Northern Blot Experiments*—Northern blot analyses were performed as described (49) using RNA isolated from *B. subtilis* wild-type cells before (control) and 10 min after treatment with 50 μM NaOCl, 1 mM diamide and 100 μM CHP, respectively. Hybridizations specific for *ohrA, nfrA, cysK, katA, ohrA, azoR1, catE,* and *yitJ* were performed with the digoxigenin-labeled RNA probes synthesized *in vitro* using T7 RNA polymerase from T7 promoter containing internal PCR products of the respective genes using the primer sets described previously (23, 25, 35) and the primer pairs yitJ-for, 5′ CCGAACAGCAGTCTTCCTTC 3′ and yitJ-T7-rev, 5′ CTAATACGACTCACTATAGGGAGACCGTTTTACCGCTTTATCCA 3′ for *yitJ*.

## RESULTS

*Determination of the Growth-inhibitory Concentration of NaOCl in B. subtilis*—At first we determined the concentration that inhibited the growth of *B. subtilis* wild-type cells. Exposure of cells to 50 μM NaOCl stress caused a lag in growth for 60 min and then growth was resumed with a similar growth rate as the untreated control (Fig. 1). This growth profile is very similar to

that of diamide (26) indicating that cells are able to detoxify the oxidant and to repair the protein damage within this time frame. Growth of *B. subtilis* is completely inhibited by 100 μM NaOCl.

*Transcriptome Analysis of the NaOCl Stress Response in B. subtilis*—To analyze the mode of action of NaOCl in *B. subtilis*, we conducted genome-wide transcriptome analyses of cells treated for 10 min with 50 μM NaOCl stress. Genes that were >3-fold up-regulated and down-regulated by NaOCl were sorted according to the known stress regulons in supplemental Tables S1 and S2. The transcriptome data revealed the significant induction of 430 genes and the repression of 400 genes by NaOCl stress in three biological transcriptome replicates. Representative genes of the most strongly up-regulated genes and regulons are listed in supplemental Table S3 and visualized in the corresponding diagram in Fig. 2. Transcriptional induction of selected thiol-stress specific genes by NaOCl, diamide and CHP was verified by additional Northern blot analyses (Fig. 3). In the following sections we have sorted the transcriptome datasets into thiol- and oxidative stress specific and general stress-induced regulons.

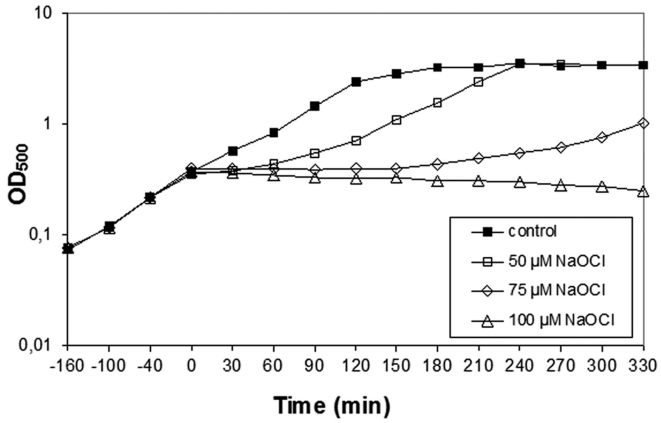


FIG. 1. **Growth curves in response to sub-lethal concentrations of NaOCl stress in *B. subtilis*.** *B. subtilis* wild type was grown in minimal medium to an $OD_{500}$ of 0.4 and exposed to 50, 75, and 100 μM of NaOCl indicated by time point zero.

*Induction of the CtsR and Spx Regulons by NaOCl Stress is Indicative of Disulfide Stress*—The microarray data showed the up-regulation of the thiol- or electrophile-stress specific CtsR and Spx regulons in *B. subtilis*. Among the CtsR and Spx regulons, the *clpE* (28-fold), *trxA* and *nfrA* (40-fold) genes displayed the highest induction ratios. The fold-changes of Spx-controlled genes are similar to diamide stress as verified by the Northern blots (Fig. 3). Because the Spx and CtsR regulons are generally induced by electrophiles, the global response to NaOCl is indicative of disulfide stress (23, 50). In contrast, the CymR regulon that functions in Cys biosynthesis (51) was strongly up-regulated by RES, but not by NaOCl stress. Among the CymR regulon genes, only *cysK* was 3-fold induced by NaOCl stress. This indicates that NaOCl probably does not deplete the pool of the redox buffer cysteine in *B. subtilis*.

*Induction of the S-box Regulon by NaOCl Stress Indicates Methionine Starvation*—Interestingly, the S-box regulon genes that are regulated by an S-adenosyl methionine riboswitch mechanism were induced by NaOCl stress (supplemental Table S1, Fig. 3). The S-box regulon is induced by methionine starvation when S-adenosyl methionine levels are low. The S-box regulon gene products function in methionine biosynthesis (52–55). The microarray data showed the induction of the methionine synthases encoding *metE* (5,3-fold),

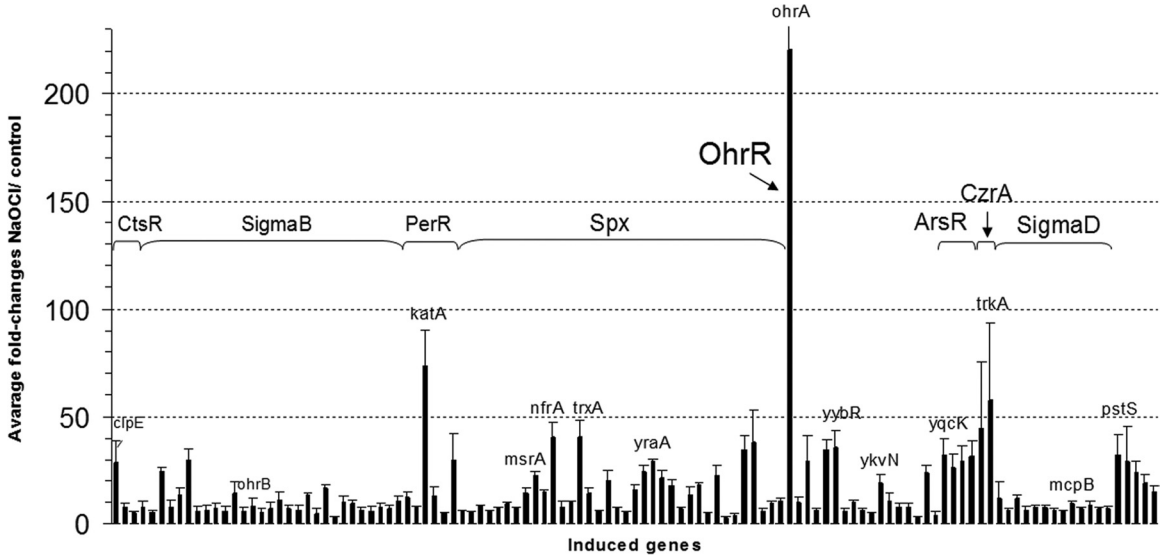


FIG. 2. **Transcriptome changes of NaOCl-induced regulons (CtsR, Spx, PerR, OhrR, ArsR, CzrA, SigmaD, and SigmaB) and of the *pstSCAB* operon.** Fold-changes are average induction ratios of genes induced in NaOCl-treated cells *versus* untreated cells calculated from three transcriptome replicates with standard deviations given as errors bars. Shown are only representative genes of each regulon that are more than fivefold induced by NaOCl in supplemental Tables S1 and S3.

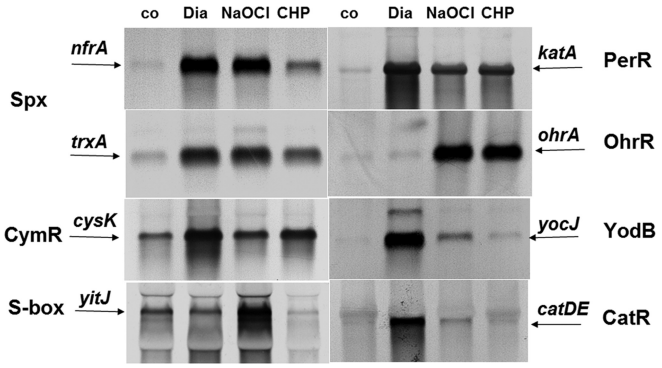


FIG. 3. **Northern blot analysis of selected thiol-stress specific genes of the Spx, CymR, S-box, PerR, OhrR, and MarR/DUF24 regulons in response to NaOCl, diamide, and CHP stress.** Transcript analysis of *nfrA, trxA*, and *katA* indicates the induction of the Spx and PerR-regulons by NaOCl and diamide stress. The CymR-controlled *cysK* gene is strongly induced by diamide. The S-box regulon gene *yitJ* responds most strongly to NaOCl stress. The *ohrA* gene is controlled by the OhrR repressor and strongly induced by NaOCl and CHP. The YodB and CatR-controlled *azoR1* and *catDE* genes are strongly up-regulated by diamide. Cells were grown to an $OD_{500}$ of 0.4 and harvested before (control conditions, co) and 10 min after exposure to 50 $\mu$M NaOCl, 100 $\mu$M CHP, or 1 mM diamide. The RNA isolation and Northern blot hybridization was performed as described in the Methods section. The arrows point toward the sizes of the specific transcripts.

*yxjG* (2,5-fold), and *yxjH* genes (2-fold), the *metIC* operon (3–4-fold) encoding cystathionine $\gamma$-synthase and $\beta$-lyase that are involved in cystathionine and homocysteine biosynthesis, the *yoaD* gene (3,6-fold) that encodes a 3-D-phosphoglycerate dehydrogenase required for serine biosynthesis and the *yitJ* gene (7,4-fold) that encodes a bifunctional homocysteine S-methyltransferase in the N-terminal part and 5,10-methylenetetrahydrofolate (N5,N10-THF) reductase in the C-terminal part (see Fig. 7). The NAD(P)H-dependent N5,N10-THF reductase activity is required to reduce N5,N10-THF to 5-methyltetrahydrofolate (N5-THF) as methyl-group donor for the methionine synthase MetE (56). The *cysH* operon that encodes gene products for sulfur assimilation and cysteine biosynthesis and the *metK* gene encoding a S-adenosyl methionine synthetase were repressed in the transcriptome by NaOCl stress. The *cysH* operon belongs also to the CymR regulon and is rather induced by cysteine starvation than by methionine starvation (57). The *metK* gene displayed also a drop of expression at later time points upon methionine starvation in previous studies (52). Thus, *metK* and *cysH* are not induced by NaOCl stress in contrast to other S-box regulon genes listed above.

*Induction of the PerR-dependent Oxidative Stress Response by NaOCl Stress*—NaOCl caused the induction of the oxidative stress specific PerR regulon genes *katA* (73-fold) and *ahpCF* (7–13-fold) (Figs. 2 and 3). The PerR regulon genes were similar strongly induced by NaOCl and diamide indicating that strong oxidants that cause disulfide stress lead probably to oxidation of the conserved Cys residues in the structural Zn-binding site as confirmed by the liquid chromatography (LC)-MS/MS results (Table I).

*Induction of the OhrR-controlled OhrA Peroxiredoxin by NaOCl Stress*—Interestingly, the *ohrA* gene was most strongly up-regulated (220-fold) in the transcriptome by NaOCl. The redox-sensing OhrR repressor controls the OhrA peroxiredoxin that confers resistance to CHP (6, 7). The Northern blots show that derepression of *ohrA* transcription occurs by CHP and NaOCl stress at similar levels (Fig. 3). These data suggest that OhrR is a specific determinant of the response to NaOCl and ROOH.

*Induction of Selective RES-specific MarR/DUF24 Regulons by NaOCl Stress*—We have shown that RES are sensed by members of the redox-sensing MarR/DUF24 family. The YodB and CatR repressors are specific sensors for quinones and diamide (7, 24–26, 50). The transcriptome and Northern blot results showed the induction of the YodB-regulon genes *azoR1* (10-fold), *yodB* (3-fold), and *yodC* (5-fold) by NaOCl. The CatR-controlled *catDE* operon was threefold induced by NaOCl. The inductions of the YodB and CatR regulons by NaOCl are much lower as by diamide and quinones (Fig. 3) confirming the specific roles of the azoreductases and dioxygenases in detoxification of diamide and quinones. In addition, the genes encoding further DUF24-like redox sensors, *yybR* (35-fold), *ykvN* (19-fold), *ydzF* (6-fold), and *ydeP* (6-fold) were induced by NaOCl stress indicating that these respond probably to disulfide stress via thiol-based redox switches. The formaldehyde-sensing DUF24-type regulator HxlR controls the *hxlAB* operon encoding the enzymes of the ribulose-5-monophosphate (RuMP) pathway (58). The *hxlAB* operon was 8-fold induced by NaOCl stress.

*Induction of Metal Ion Efflux Systems, Motility and Chemotaxis by NaOCl Stress*—Besides thiol- and oxidative stress responses, the CzrA, ArsR, and CsoR regulons were strongly up-regulated by NaOCl stress that control the operons for metal ion efflux systems *czcD-trkA* (32-fold), *arsR-yqcK-arsBC* (57-fold), and *yvgXYZ* (3-fold) (59–61). Furthermore, the SigmaD regulon genes for flagella assembly, motility and chemotaxis were strongly induced by NaOCl stress (23, 62). Metal ion uptake systems and SigmaD regulon genes were induced by NaOCl and RES.

*Induction of the SigmaB-dependent General Stress Response by NaOCl Stress*—In contrast to electrophiles, NaOCl stress caused the 3–15-fold induction of 52 genes belonging to the SigmaB general stress response regulon. Among the SigmaB-controlled genes, 20 genes were relatively weakly induced (3-fold) and 32 genes in the range of 5–13-fold. Representative genes of the SigmaB regulon include *dps* (5-fold), *gsiB* (8-fold), *gspA* (13-fold), *ydaST* (6-fold), *yfhK* (7-fold), *yfkM* (6-fold), *yflT* (13-fold) *ohrB* (8-fold), *ysnF* (7-fold), and *ytxGHJ* (6–13-fold). The induction of the SigmaB response might be caused as a result of starvation or even oxidative stress response caused by hypochloric acid which requires further studies. It is interesting to note that NaOCl

triggers the induction of thiol- and oxidative stress responses as well as general stress responses.

*Other Genes Induced Strongly by NaOCl Stress*—Finally, many genes with unknown functions are up-regulated in the NaOCl transcriptome (supplemental Table S1). The putative $Na^+/H^+$ antiporter *nhaX* (30-fold) and the major facilitator superfamily encoding *ybcLM* operon (42-fold) could be involved in sodium efflux. The high induction of the *pstSCAB* operon (30-fold) by NaOCl might be PhoPR-independent because other PhoPR-regulon genes were not induced, such as *phoA*, *phoB,* and *phoD* encoding alkaline phosphatases and phosphodiesterases. Finally, the *yhdJ* gene encoding the putative GCN5-N-acetyltransferase was 67-fold induced by NaOCl.

*Repression of the Stringent Controlled RelA-regulon by NaOCl Stress*—There are 400 genes in the transcriptome datasets that displayed more than 3-fold decreased expression ratios in response to NaOCl stress (supplemental Table S2). Among the repressed genes are the stringent controlled RelA regulon genes involved in translation, ATP generation, cell wall biosynthesis, and turnover. The PurR and RyrR regulons controlling purine and pyrimidine biosynthesis were repressed by NaOCl as result of the slower growth rate. The osmostress-responsive uptake systems for choline and glycine betaine encoded by the *opuA, opuB*, and *opuC* operons were strongly repressed by NaOCl stress (63).

*Hierarchical Clustering Analyses for RES and NaOCl Indicates a Disulfide Stress Signature of NaOCl*—Next, we performed a hierarchical clustering analysis using selected transcriptome datasets for diamide (45), MHQ (46–47), catechol (47), formaldehyde, methylglyoxal (23), and NaOCl. In total, 630 genes were selected for the clustering analysis that showed inductions of at least threefold in any of these transcriptome datasets (supplemental Table S4). The complete cluster can be arranged in 14 major groups of genes which share a similar expression profile by electrophiles and NaOCl (Fig. 4). The cluster analysis confirmed the common induction of the CtsR, Spx (node 9), ArsR, CzrA, and SigmaD regulons (nodes 11, 12) by RES and NaOCl as indicator for disulfide stress. The strong induction of the CymR regulon by RES but not by NaOCl is visualized in cluster 13. The quinone and diamide-specific MarR/DUF24 regulons controlled by YodB, CatR, and MhqR clustered with the PerR regulon in nodes 6, 8, and 10. The aldehyde-specific HxlR, AdhR, LexA regulons and the formate uptake system and formate dehydrogenase encoding *yrhFG* and *yrhDE* operons (23) clustered in nodes 11 and 14. The NaOCl-specific inductions of the OhrR and SigmaB regulons, the *ydzF* and *yfkN* genes encoding DUF24-family regulators and the *pstSCAB* operon are shown in clusters 1, 3, 4. In conclusion, the transcriptome comparisons showed that NaOCl elicits a Spx, CtsR-, and PerR-controlled disulfide and oxidative stress response and a selective OhrR- and SigmaB response in *B. subtilis*.

*Thiol-redox Proteomics Identifies GapA, MetE, MtnA, LeuC and PurQ as Reversibly Oxidized Proteins by NaOCl Stress*—Next, we were interested in the changes in the thiol-redox proteome by NaOCl stress to identify proteins with reversible thiol modifications. In brief, reduced thiol groups were blocked with IAM and reversibly oxidized proteins were reduced and labeled using the fluorescence dye BODIPY FL $C_1$-IA (21, 38). The fluorescence-labeled proteins representing the disulfide proteome were separated using two-dimensional gels and the fluorescence image (red) overlaid with the Coomassie-stained protein amount image (green) (Fig. 5*A*, 5*B*). The oxidation ratios were quantified as BODIPY-fluorescence levels *versus* protein amount levels of the reversibly oxidized proteins (Fig. 5*C*). In agreement with previous studies, proteins that form disulfides under control conditions include Adk, AhpC, AccB, Eno, Tpx, PdhD, GuaB, CysH, CysJ (YvgR), LeuC, YceC, and YumC (Fig. 5*A*) (21, 22). The identities of these oxidized proteins were verified using MALDI-TOF-TOF MS/MS (supplemental Figs. S1*A–P*).

Surprisingly, we did not detect a strong increase of reversible thiol-oxidations in the redox proteome in many cytoplasmic proteins after treatment of cells with 50 $\mu$M NaOCl stress. Instead, NaOCl rather caused specific oxidation of few selective proteins, including GapA, MetE, MtnA, LeuC, and PurQ (Fig. 5*B*, 5*C*). The glyceraldehyde-3-phosphate dehydrogenase (GapA) was identified as most strongly oxidized protein with a 10-fold increased fluorescence/protein ratio (Fig. 5*B*, 5*C*). The redox proteome analysis revealed also strongly increased oxidation ratios for the cobalamin-independent methionine synthase MetE. Furthermore, the methylthioribose-1-phosphate isomerase MtnA (YkrS) is oxidized by NaOCl stress that is involved in methionine biosynthesis *via* the salvage pathway (see Fig. 7).

*Identification of Proteins with Intramolecular Disulfides Under Control and NaOCl Stress Conditions Using Shotgun-LC-MS/MS Analyses*—We were interested to identify proteins with reversible thiol-oxidations, including intramolecular disulfides, *S*-cysteinylations, and S-bacillithiolations under NaOCl stress conditions. We are aware that we exclude the identifications of intramolecular disulfides of proteins with Cys residues that are separated by tryptic digestion resulting in cross-linked intermolecular disulfides after enzymatic digestion. Alkylated protein extracts of control and NaOCl-treated cells were separated using nonreducing SDS-PAGE, tryptically in-gel digested and analyzed using LTQ-Orbitrap-Velos mass spectrometry as described in the Methods section.

Eight proteins with intramolecular disulfides were identified in wild-type proteome samples at control and NaOCl stress conditions, including Adk, CysJ (YvgR), GltA, PdhD, TopA, YutI, YdjI, and Zwf (Table I and supplemental Figs. S2*A–2K*). Adk, PdhD, and CysJ were detected also in the redox proteome as reversibly oxidized proteins under control conditions (Fig. 5*A*). The dihydrolipoamide dehydrogenase E3 sub-

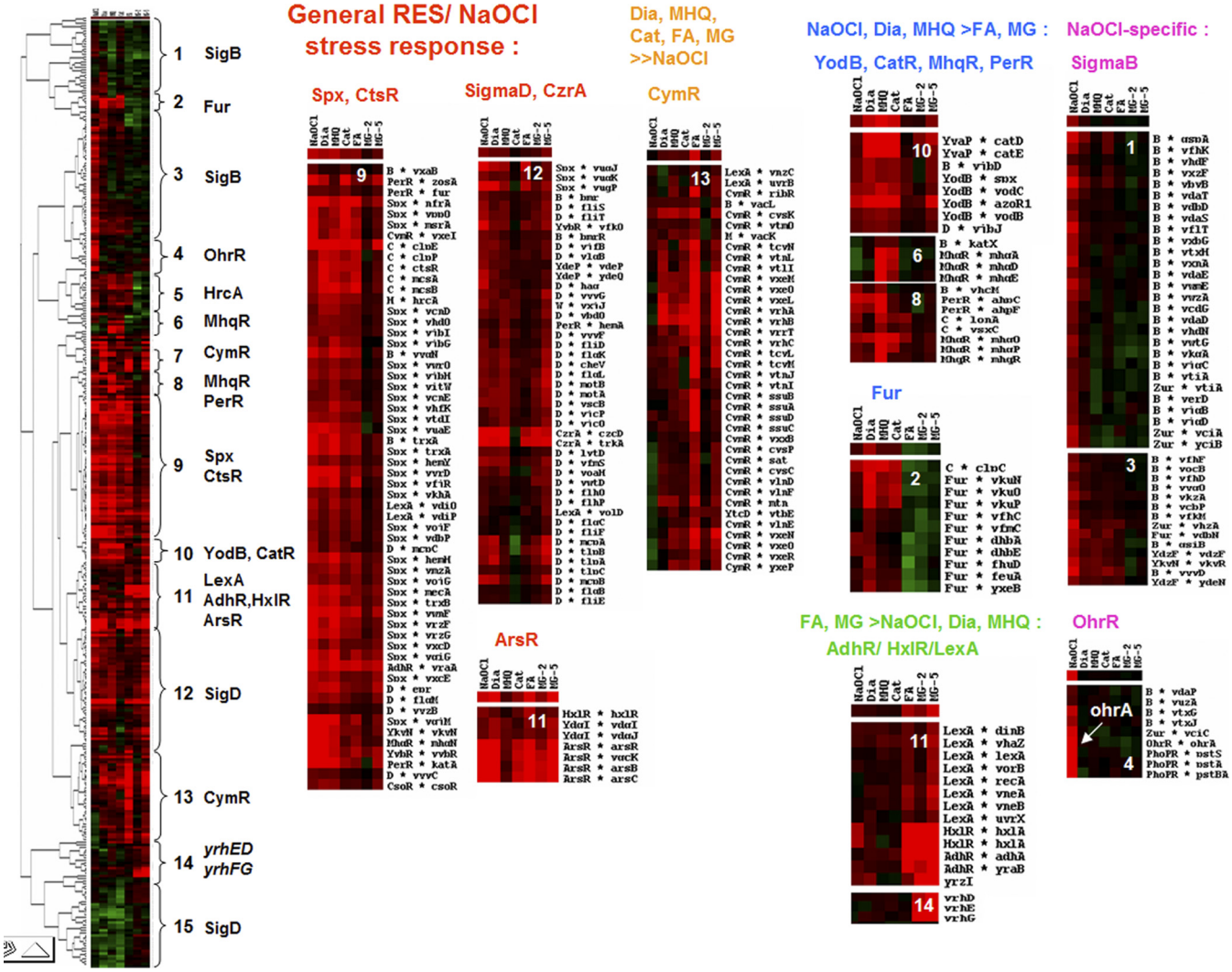


FIG. 4. **Hierarchical clustering analysis of RES and NaOCl induced gene expression profiles.** Log2-fold changes of gene expression ratios were clustered for 1 mM diamide (Dia), 2.4 mM catechol (Cat), 0.5 mM methylhydroquinone (MHQ), 1 mM formaldehyde, 2.8 mM and 5.6 mM methylglyoxal (MG-2 and MG-5), and 50 $\mu$M NaOCl stress using the Treeview software. The cluster analysis resulted in 14 different nodes that are enriched for RES and NaOCl-induced regulons (CtsR, Spx, ArsR, CzrA, CsoR, SigmaD), the RES-specific CymR regulon, quinone-responsive regulons (PerR, YodB, CatR (YvaP), MhqR), aldehyde-responsive regulons (HxlR, AdhR, LexA) and NaOCl-specific regulons (SigmaB, OhrR). For the cluster analysis 630 genes were selected as listed in supplemental Table S4 that are induced by RES and NaOCl stress. Red indicates induction and green repression under the stress specific conditions.

unit of the pyruvate dehydrogenase complex (PdhD) forms an active site Cys47-Cys52 intramolecular disulfide used for oxidation of the dihydrolipoamide to lipoamide (64). The adenylate kinase Adk and the topoisomerase 1 (TopA) form intramolecular disulfides in Zn binding sites (Table I). Further proteins with intramolecular disulfides include those with Fe-S clusters or Fe-binding sites, such as the glutamate synthase large subunit GltA (GOGAT), the sulfite reductase flavoprotein alpha subunit CysJ (YvgR) and the Fe-S cluster assembly protein YutI.

Three redox-sensitive proteins were identified that are oxidized to intramolecular disulfides only under NaOCl stress conditions, including GapA, PerR, and Spx (Table I). GapA is most strongly oxidized in response to NaOCl stress in the redox proteome (Fig. 5*B*). GapA was neither oxidized in the redox proteome (Fig. 5*A*) nor during tryptic digestion in control extracts indicating that no oxidation occurred during our sample preparation protocol. The intramolecular $C_{152}$-$C_{156}$ disulfide bond in GapA's catalytic center was detected as triply charged peptide YDAANHDVISNASC$_{152}$(-2)TTNC$_{156}$LAPFAK at an m/z = 842,0466 (supplemental Fig. S2*B*).

The intramolecular disulfides for Spx and PerR were identified only in cell extracts of NaOCl-treated *bshA* mutant cells. The redox-sensing regulator Spx is activated by a thiol-disulfide redox switch in the N-terminal $C_{10}xxC_{13}$ motif in response to diamide stress (65, 66). This $C_{10}$-$C_{13}$ intramolecular disulfide was identified as doubly charged peptide $M_1$(+16)VTLYTSPSC$_{10}$(-2)TSC$_{13}$R at an *m/z* = 781,8378 in NaOCl-treated cells (supplemental Fig. S2*F*). The peroxide-

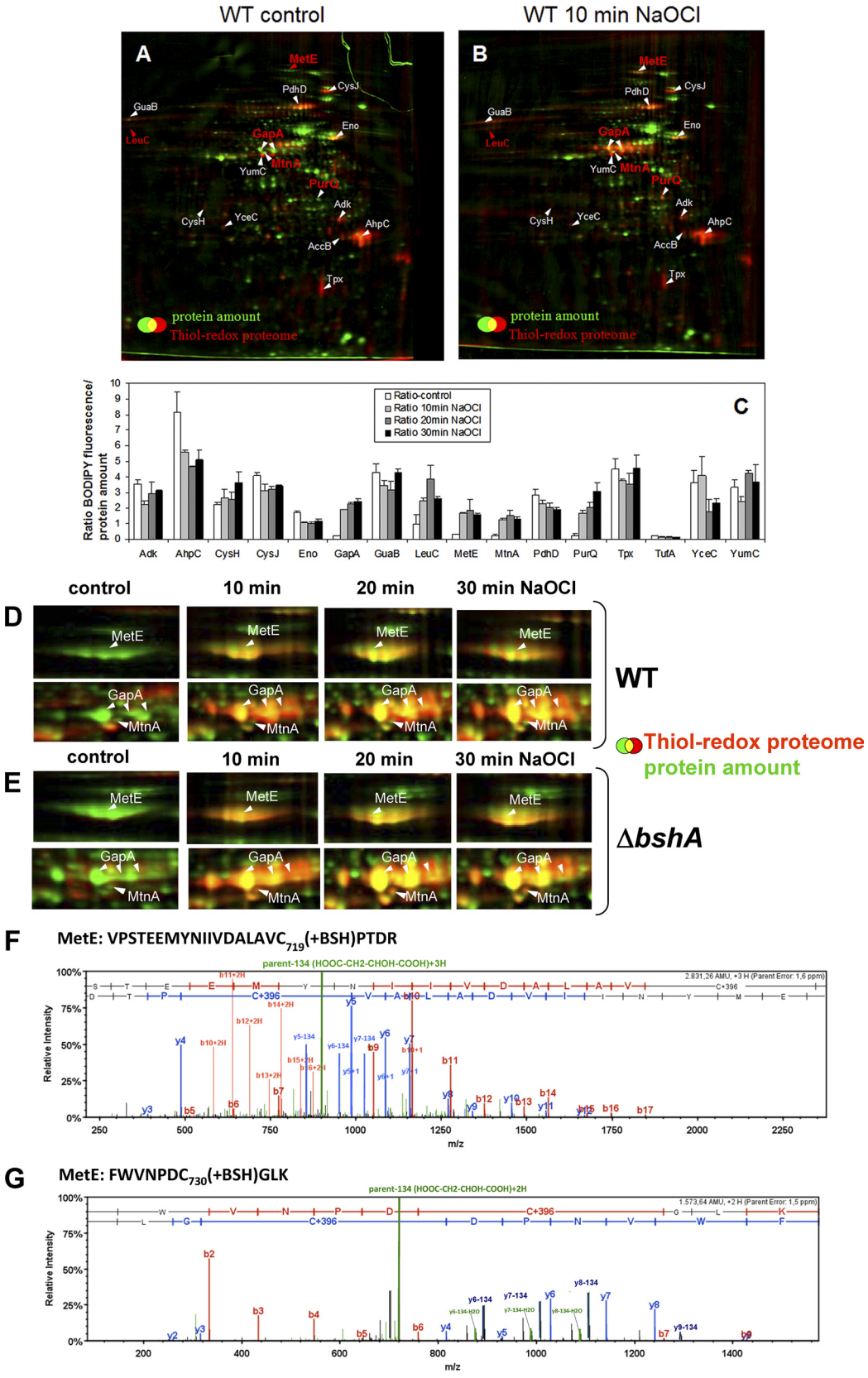
WT control
WT 10 min NaOCl
A
B
MetE
PdhD
CysJ
GuaB
LeuC
GapA
Eno
YumC
MtnA
PurQ
Adk
CysH
YceC
AhpC
AccB
Tpx
protein amount
Thiol-redox proteome
C
Ratio BODIPY fluorescence/ protein amount
Ratio-control
Ratio 10min NaOCl
Ratio 20min NaOCl
Ratio 30min NaOCl
Adk AhpC CysH CysJ Eno GapA GuaB LeuC MetE MtnA PdhD PurQ Tpx TufA YceC YumC
control
10 min
20 min
30 min NaOCl
D
WT
Thiol-redox proteome
protein amount
E
ΔbshA
F
MetE: VPSTEEMYNIIVDALAVC719(+BSH)PTDR
parent-134 (HOOC-CH2-CHOH-COOH)+3H
Relative Intensity
m/z
G
MetE: FWVNPDC730(+BSH)GLK
parent-134 (HOOC-CH2-CHOH-COOH)+2H
Relative Intensity
m/z

sensing PerR repressor is inactivated in response to hydrogen peroxide by iron-catalyzed His-oxidation (14). The intramolecular disulfide was detected in the structural Zn-binding site of PerR as doubly charged peptide LEIYGVC$_{136}$QEC$_{139}$(-2)SK at an *m/z* = 685,3092 (supplemental Fig. S2*E*). This suggests that PerR senses disulfide stress probably via oxidation of the Cys residues in the Zn binding site.

*Identification of S-bacillithiolations in OhrR, MetE, YxjG, PpaC, SerA, and YphP in the Proteome of NaOCl-treated Cells Using Shotgun-LC-MS/MS Analysis*—The OhrR repressor is inactivated by an *S*-thiolation mechanism including cysteine and BSH in response to CHP (7, 19). Our data showed that NaOCl stress also inactivates the OhrR repressor because *ohrA* transcription was derepressed. Thus, we analyzed whether OhrR forms mixed disulfides with cysteine or BSH in response to NaOCl. Because OhrR is a low abundant regulatory protein, a FLAG-epitope-tagged OhrR protein was enriched using immunoprecipitation (IP) from NaOCl-treated cells as in previous studies (19). Purified OhrR-FLAG protein was tryptically digested and analyzed by LTQ-Orbitrap MS/MS analysis as described in the Methods section. In protein samples containing OhrR-FLAG protein from NaOCl-treated cells, the Cys15-peptide was identified as triply charged peptide at an *m/z* = 684.98 containing the additional mass of BSH (+396 Da) (supplemental Fig. S3*A*, Table II). This indicates that OhrR is inactivated by an *S*-bacillithiolation mechanism in response to NaOCl stress. To verify that only Cys15 of OhrR is involved in redox-sensing of NaOCl stress, we analyzed *ohrA* transcription in an *ohrRC15S* mutant (34). The Northern blot results in supplemental Fig. S3*A* indicate that *ohrA* transcription is completely abolished in the *ohrRC15S* mutant. This confirms that regulation of *ohrA* transcription requires only inactivation of the redox-sensing Cys15 of OhrR.

Next, we searched our LC-MS/MS results obtained from whole proteome tryptic digests of NaOCl-treated cells for *S*-thiolation modifications. We identified five cytoplasmic proteins that were modified by *S*-bacillithiolation, including two methionine synthase paralogs MetE and YxjG (Fig. 5*F*, 5*G*, supplemental Fig. S3B, 3C, Table II), the inorganic pyrophosphatase PpaC (supplemental Fig. S3*D*, Table II), the 3-D-phosphoglycerate dehydrogenase SerA (supplemental Fig. S3*E*, Table II) and the thiol-disulfide oxidoreductase YphP (supplemental Fig. S3*F*, Table II). The MetE protein was identified as specific target for reversible thiol-oxidation by NaOCl stress in the redox proteome (Fig. 5*B*, 5*C*). Moreover, MetE, PpaC and SerA have been shown to be modified by S-cysteinylations in response to diamide stress (67).

For MetE we detected the triply charged peptide VPSTEEMYNIIVDALAVC$_{719}$(+BSH)PTDR at an *m/z* = 944.7604 and the doubly charged peptide FWVNPDC$_{730}$(+BSH)GLK at an *m/z* = 787,8297 containing the additional mass of BSH (+396 Da) at Cys719 and Cys730 (Fig. 5*F*, 5*G*; supplemental Fig. S3*B*, Table II). In addition, the triply charged Cys730 peptide with an *S*-cysteinylation modification was identified as peptide FWVNPDC$_{730}$(+Cys)GLK at an *m/z* = 433,1952 containing the additional mass of Cys (+119 Da) (supplemental Fig. S3*B*; Table II). Interestingly, the CID MS/MS spectra of the bacillithiolated MetE peptides revealed a characteristic loss of malate from the precursor ions and from abundant y-fragment ions as indicated by the loss of 134 Da. The precursor ions minus 134 Da are most abundant in the MS/MS spectra of the bacillithiolated peptides identified for MetE, PpaC and SerA. Thus, the bacillithiolated and cysteinylated Cys730 peptides of MetE showed different MS/MS fragment ion spectra (supplemental Fig. S3*B*). Moreover, the abundance of the precursor ions minus malate leads also to decreased intensities of the b and y ions in the MS/MS spectra of the bacillithiolated PpaC and SerA peptides (supplemental Fig. S3D, 3E).

For YxjG, we detected the triply charged peptide YVSLDQLC$_{341}$(+IAM)LSPQC$_{346}$(+BSH)GFASTEEGNK at an *m/z* = 981,4183 with the additional mass of 396 Da at Cys346 (supplemental Fig. S3*C*, Table II). YxjG is homolog to the C-terminal part of MetE and the essential Zn-binding Cys730 residue of MetE aligns with Cys346 in YxjG. This suggests that also Cys346 of YxjG could be essential for methionine synthase activity. Thus, homolog active site Cys residues are S-bacillithiolated in the paralogous methionine synthases MetE and YxjG.

FIG. 5. **ABC. The thiol-redox proteome (*red*) in comparison to the protein amount image (*green*) at control conditions (*A*) and after exposure to 50 μM NaOCl (*B*) in the wild type.** Reduced protein thiols in cell extracts were alkylated with IAM followed by reduction of oxidized protein thiols with TCEP and labeling with BODIPY FL C$_1$-IA. Proteins with reversible thiol-modifications in the control and NaOCl redox proteome are labeled in white and newly oxidized proteins in NaOCl-treated cells are labeled in red. The oxidized proteins were identified by MALDI-TOF-TOF MS/MS as shown in detail in supplemental Fig. S1*A–P*. *C*, The fluorescence/protein amount ratios are quantified as oxidation ratios at control conditions (control) and 10, 20, and 30 min after exposure to 50 μM NaOCl stress as shown in the diagram.

**DEFG. Close-ups of the main NaOCl-sensitive proteins MetE and GapA in the thiol-redox proteome of the wild type (*D*) and *bshA* mutant (*E*) and CID MS/MS spectra of the S-bacillithiolated Cys719 and Cys730 peptides of MetE (*F*, *G*).** Figs. *D* and *E* show sections of reversibly oxidized proteins after NaOCl stress in the thiol-redox proteome (red) in comparison to the protein amount image (*green*) at control conditions (co) and 10, 20, and 30 min after exposure to 50 μM NaOCl. Figs. *F* and *G* show the CID MS/MS spectra of the S-bacillithiolated Cys719-and Cys730-peptides of MetE identified in the wild-type proteome using LTQ-Orbitrap-Velos mass spectrometry as described in the Methods section. The MS/MS spectra show the characteristic abundant precursor ions that have lost malate indicated by parent-134 (HOOC-CH$_2$-CHOH-COOH). The Xcorr and ΔCn scores and peptide masses are listed in Table II and the corresponding b and y fragment ion series for the modified peptides are given in detail in supplemental Fig. S3*B*.

TABLE I

***Proteins with intramolecular disulfides identified at control and NaOCl stress conditions.*** *Cytoplasmic proteins were harvested in IAM-urea/thiourea-buffer, separated using SDS-PAGE, tryptically digested and analyzed in a LTQ Orbitrap-Velos mass spectrometer as described in the Methods section. Peptides with intramolecular disulfides that showed a mass difference of Cys-2 Da were identified for Adk, GltA, CysJ, PdhD, TopA, YdjI, YutI, and Zwf in control and NaOCl samples. The table includes the m/z of the precursor ions, charges, Xcorr and ΔCn scores of the disulfide linked peptides. The complete CID MS/MS spectrum of all peptides and the b and y fragment ion series are given in supplemental Fig. S2A–K as indicated in column SI-Fig.*

| SI-Fig. | Protein | Function | Redox-active Cys | Disulfide-Peptide | *m/z* precursor ion | XCorr-score | ΔCn score | Charge |
|---|---|---|---|---|---|---|---|---|
| S2A | Adk[b] | Adenylate kinase | Zn-binding: Cys130,133, 150,153 | $IC_{130}SVC_{133}$(-2)GTTYHLVFNPPK | 938,9590 | 4,6515 | 0,6794 | 2 |
| S2B | **GapA**[a,b] | Glyceraldehyde 3-phosphate dehydrogenase | Cys152 redox-active catalytic site | YDAANHDVISNASC$_{152}$(-2) TTNC$_{156}$LAPFAK | 842,0466 | 5,8694 | 0,7600 | 3 |
| S2C | GltA | Glutamate synthase large subunit | 3Fe-4S: C113, 1119, 1124 | $AC_{1119}$(-2) HLDTC$_{1124}$PVGVATQNPELR | 674,6567 | 5,2172 | 0,7056 | 3 |
| S2D | PdhD[b] | dihydrolipoamide dehydrogenase E3 subunit of pyruvate dehydrogenase | Cys47 and Cys52 redox-active disulfide as catalytic centre | ATLGGVC$_{47}$(-2)LNVGC$_{52}$IPSK | 765,3950 | 3,6256 | 0,5999 | 2 |
| S2E | **PerR**[a] | Fur-family repressor of the peroxide regulon | Zn-binding site:Cys96,99, 136,139 | LEIYGVC$_{136}$QEC$_{139}$(-2)SK | 685,3092 | 2,6948 | 0,7523 | 2 |
| S2F | **Spx**[a] | Regulator of the disulfide stress response | Cys10, 13 redox-active sites | $M_1$(+16)VTLYTSPSC$_{10}$(-2)TSC$_{13}$R | 781,8378 | 2,9770 | 0,7398 | 2 |
| S2G | TopA | DNA topoisomerase 1 | 3 Zn-fingers: Cys579,582, 599,605 | | | | | |
| | | | Cys619,622,641,647 Cys660,663,680,683 | C$_{619}$PSC$_{622}$(-2)GEGNIVER | 631,2697 | 2,3857 | 0,7171 | 2 |
| S2H | YdjI | Unknown | Unknown | TGEANFC$_{315}$PNC$_{318}$(-2)GQK | 683,7802 | 2,8661 | 0,6388 | 2 |
| S2I | YutI | Putative nitrogen fixation protein, Fe-S cluster assembly or repair | Cys79 and Cys82 Fe-S-cluster binding | LLGAC$_{79}$GSC$_{82}$(-2)PSSTITLK | 774,8928 | 4,3033 | 0,6283 | 2 |
| S2J | YvgR[b](CysJ) | Sulfite reductase [NADPH] flavoprotein alpha-component | Cys427 and Cys431 probably Fe-binding | GVC$_{427}$(-2)SILC$_{431}$AER | 524,7494 | 2,1040 | 0,5121 | 2 |
| S2K | Zwf | Glucose-6-phosphate dehydrogenase | Unknown | LDYC$_{407}$(-2)SNC$_{410}$NDELNTPEAYEK | 1109,9501 | 4,8708 | 0,8275 | 2 |

[a] The intramolecular disulfide of GapA was detected in NaOCl-treated wild-type and *bsh* mutant cells and the disulfides for PerR and Spx were detected in NaOCl-treated *bsh* mutant cells.

[b] Adk, GapA, PdhD, and YvgR (CysJ) were also identified in the redox proteome as reversible oxidized proteins (Fig. 5*A*, 5*B*).



10.1074/mcp.M111.009506–11

TABLE II

***Proteins with S-Bacillithiolations and S-Cysteinylations identified in NaOCl-treated cells.*** *Cytoplasmic proteins of the wild type were harvested in IAM-buffer, separated using SDS-PAGE, tryptically digested and analyzed in a LTQ Orbitrap-Velos™ mass spectrometer as described in the Methods section. Peptides with S-bacillithiolations were identied for OhrR, MetE, YxjG, PpaC, SerA, and YphP indicated by the additional mass of 396 Da. Peptides with S-cysteinylations were identified for MetE and PpaC with a mass difference of 119 Da. The table includes the m/z of the precursor ions, charges, Xcorr, and ΔCn scores of the S-thiolated peptides. The complete CID MS/MS spectrum of all peptides and the b and y fragment ion series are given in supplemental Fig. S3A–F as indicated in column SI-Fig.*

| SI-Fig. | Protein | Function | Redox-active Cys | S-thiolated Peptide | *m/z* precursor ion | XCorr-score | ΔCn score | Charge |
|---|---|---|---|---|---|---|---|---|
| S3A | OhrR | Redox-sensing MarR-type repressor for organic hydroperoxide resistance | Cys15 redox-sensing | LENQLC$_{15}$(+BSH)FLLYASSR | 684,9800 | 2,9444 | 0,5816 | 3 |
| S3B | MetE[a] | Cobalamin-independent methionine synthase | Cys 647, 730 essential, Zn-binding active site in *B. sub.* | VPSTEEMYNIIVDALAVC$_{719}$(+BSH)PTDR | 944,7604 | 4,9737 | 0,7545 | 3 |
| | | | Cys719 non-essential, S-cysteinylated by diamide in *B. sub.* | FWVNPDC$_{730}$(+BSH)GLK | 787,8297 | 2,8014 | 0,6097 | 2 |
| | | | Cys645 non-essential, S-glutathionylated in *E. coli* | FWVNPDC$_{730}$(+Cys)GLK | 433,1952 | 3,2330 | 0,5435 | 3 |
| S3C | YxjG | Cobalamin-independent methionine synthase | Cys251, 346 homolog to Zn-binding Cys647, 730 in MetE of *B. sub.* | YVSLDQLC$_{341}$(+IAM)LSPQC$_{346}$-(+BSH)GFASTEEGNK | 981,4173 | 4,9686 | 0,7521 | 3 |
| S3D | PpaC | inorganic pyrophosphatase | Cys158 | SPTC$_{158}$(+BSH)TDQDVAAAK | 851,8456 | 3,4552 | 0,8838 | 2 |
| | | | S-cysteinylated by diamide in *B. sub.* | SPTC$_{158}$(+Cys)TDQDVAAAK | 713,3041 | 3,2977 | 0,8356 | 2 |
| S3E | SerA | 3-D-phosphoglycerate dehydrogenase | Cys410 S-cysteinylated by diamide in *B. sub.* | ISSSESGYDNC$_{410}$(+BSH)ISVK | 992,9086 | 3,6448 | 0,8507 | 2 |
| S3F | YphP | Thiol-disulfide isomerase | Cys53 redox-active | AEGTTLVVVNSVC$_{53}$(+BSH)GC$_{55}$-(+IAM)AAGLAR | 815,3752 | 4,077 | 0,6036 | 3 |

[a] MetE was also identified as reversibly oxidized in the redox proteome after NaOCl stress. The identification of the essential Zn-binding ligands Cys647 and 730 of *B. subtilis* MetE is based on similarity to the *E. coli* MetE enzyme and derived from the UniprotKB database entry P80877.

The inorganic pyrophosphatase PpaC was *S*-bacillithiolated at Cys158 and the same site was also *S*-cysteinylated by diamide (67). For PpaC the Cys158-containing doubly charged peptide $SPTC_{158}$(+BSH)TDQDVAAAK was detected at an *m/z* = 851,8456 Da with the additional mass of 396 Da (supplemental Fig. S3*D*, Table II). We also detected the doubly charged S-cysteinylated Cys158-containing peptide of PpaC $SPTC_{158}$(+Cys)TDQDVAAAK at an *m/z* = 713,3041 indicated by the additional mass of 119 Da (supplemental Fig. S3*D*, Table II). Thus, for MetE and PpaC S-bacillithiolations and S-cysteinylations were observed.

The phosphoglycerate dehydrogenase SerA was S-bacillithiolated at Cys410 in response to NaOCl stress and the same site was S-cysteinylated by diamide stress (67). The S-bacillithiolated Cys410-peptide ISSSESGYDN$C_{410}$(+BSH)ISVK was detected as doubly charged peptide at an *m/z* = 992,9086 with the additional mass of 396 Da (supplemental Fig. S3*E*, Table II).

Interestingly, the thiol-disulfide isomerase YphP (68) was identified as S-bacillithiolated at the redox-active Cys53 residue. The triply charged peptide AEGTTLVVVNSV$C_{53}$-(+BSH)G$C_{55}$(+IAM)AAGLAR was observed at an *m/z* = 815,3752 with the additional mass of 396 Da at Cys53 and the carbamidomethylation at Cys55 (supplemental Fig. S3*F*, Table II).

*The OhrA Peroxiredoxin and the BSH Redox Buffer are Essential for Protection Against NaOCl Stress*—Next, we analyzed if the growth of *ohrA* and *ohrR* mutant strains is affected by NaOCl treatment. The growth of an *ohrA* mutant was strongly impaired by 50 $\mu$M NaOCl compared with that of the wild type whereas the *ohrR* mutant was more resistant to 75 $\mu$M NaOCl (Fig. 6). Thus, the *ohrA* encoded peroxiredoxin is a specific determinant of NaOCl resistance in *B. subtilis* and perhaps involved in detoxification of this strong oxidant.

Next, we monitored the growth of *bshA* and *bshB1B2* mutants with defects in the BSH biosynthesis enzymes (35). The growth of NaOCl-treated *bshA* and *bshB1B2* mutants was strongly impaired compared with the wild type (Fig. 6). While the growth of the wild type was resumed 60 min after treatment with 50 $\mu$M NaOCl, the *bsh* mutants required 180 min to resume growth. This NaOCl-sensitive phenotype of *bsh* mutants points to a major role of BSH in NaOCl detoxification similar as glutathione (GSH) in *E. coli* (69).

Finally, we investigated whether the PerR, Spx and SigmaB regulons confer protection against NaOCl. However, the *perR* mutant that overproduces the catalase KatA and the alkylhydroperoxide reductase AhpCF was not resistant to NaOCl stress (data not shown). The *spx* mutant displayed increased sensitivities toward NaOCl stress, but the growth was also impaired under non-stress conditions due to the pleiotropic phenotype of the *spx* mutant (Fig. 6). The growth of the *sigB* mutant was only slightly impaired by NaOCl indicating perhaps a role of the SigmaB-controlled OhrA-paralog OhrB in NaOCl detoxification. These results lead to the conclusion that the OhrA peroxiredoxin and the BSH redox buffer play most essential roles in NaOCl detoxification.

*The Growth Defect in Response to NaOCl Stress can be Attributed to Methionine Limitation*—The methionine synthase MetE catalyzes the final step in the methionine biosynthesis, the chemically difficult methyl group transfer of methyltetrahydrofolate (N5-THF) to homocysteine (70) (Fig. 7). Diamide stress leads to methionine auxotrophy that is caused by MetE inactivation via *S*-cysteinylation in *B. subtilis* and *S*-glutathionylation in *E. coli* (38, 67, 70, 71). *S*-bacillithiolation of the active site Cys residues of MetE and YxjG most likely leads to enzyme inactivation and methionine auxotrophy by NaOCl stress. This methionine starvation phenotype was supported by the induction of the S-box regulon genes in the transcriptome (Fig. 7, supplemental Table S1). Using Northern blot analysis the transcriptional induction of the S-box regulon gene *yitJ* was verified during the time of starvation after exposure to 50 $\mu$M NaOCl (Fig. 7).

Furthermore, growth experiments were performed in the presence of extracellular methionine to confirm the methionine starvation phenotype. Cells were treated with of 75 $\mu$l NaOCl and 30 or 60 min later 75 $\mu$M extracellular methionine was added. The growth was resumed immediately after methionine addition (Fig. 8*A*). To control that the added methionine does not simply remove the remaining oxidants from the supernatant, the NaOCl concentrations in the culture supernatants were monitored using the FOX-assay. The results showed that 66% of NaOCl is consumed and detoxified by the cells after 30 min and 93% after 60 min supporting that the added methionine abolished the methionine starvation phenotype (Fig. 8*B*). In another experiment, cells were inoculated in minimal medium containing 75 $\mu$M methionine, grown to an $OD_{500}$ of 0.4 and treated with 75 $\mu$M NaOCl. Cells were able to grow without any lag phase in the methionine-supplemented medium after treatment with 75 mM NaOCl (Fig. 8*C*). This indicates that NaOCl stress causes methionine auxotrophy that can be abolished by methionine addition.

*B. subtilis* contains about 1 $\mu$mol/g BSH and 0.58 $\mu$mol/g Cys as redox buffers (35). To analyze whether Cys can replace BSH in post-translational modification and MetE inactivation, *bshA* mutant cells were exposed to 60 $\mu$M NaOCl and 30 and 60 min later 60 $\mu$M methionine was added. Methionine was able to restore also the growth of *bshA* mutant cells indicating that the growth defect of *bshA* mutants could be attributed to methionine auxotrophy (supplemental Fig. S4*A*). The transcriptional induction of the S-box regulon gene *yitJ* in the *bshA* mutant by 50 $\mu$M NaOCl stress supports the methionine starvation phenotype (Fig. 7). In addition, the redox proteome of NaOCl-treated *bshA* mutant cells revealed similar MetE oxidation ratios as observed for the wild type (Fig. 5E). Using the shotgun LC-MS/MS approach we identified the S-cysteinylated Cys730-peptide of MetE in the *bshA* mutant proteome (supplemental Fig. S5). These results indicate that Cys can replace BSH for post-translational modifications and inactiva-

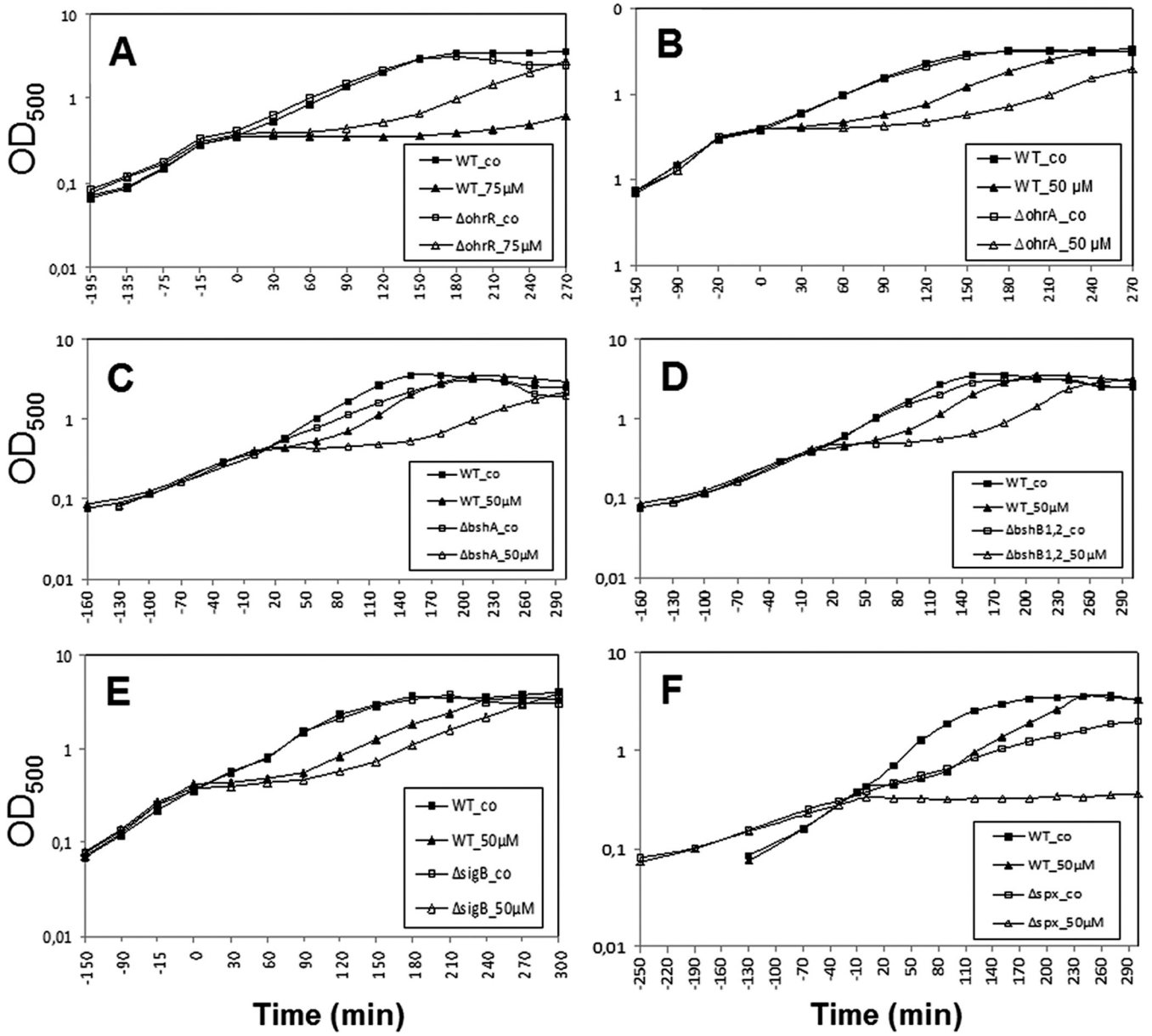


FIG. 6. **The OhrA peroxiredoxin and BSH protect cells against NaOCl toxicity.** Growth phenotype of *B. subtilis* wild type (wt) in comparison to the Δ*ohrR* (*A*), Δ*ohrA* (*B*), Δ*bshA* (*C*), Δ*bshB1,B2* (*D*), Δ*sigB* (*E*), and Δ*spx* (*F*) mutant strains that were treated with 50 or 75 µM NaOCl at an $OD_{500}$ of 0.4.

tion of MetE. However, the *bshA* mutant was strongly impaired in NaOCl detoxification and consumption compared with the wild type because about 50% of NaOCl was left in the medium after 60 min in the *bshA* mutant (supplemental Fig. S4*B*). This indicates that BSH is more efficient in NaOCl detoxification than Cys.

## DISCUSSION

Hypochloric acid is widely used as disinfectant and produced in activated macrophages by the enzyme myeloperoxidase as first defense line upon bacterial infections. Hypochloric acid is beneficial by killing invading bacteria but can result also in host tissue damage and diseases. The redox proteome in response to NaOCl has been recently studied in *E. coli* using the OxICAT approach and several redox-sensitive proteins could be identified that are sensitive to NaOCl-directed reversible oxidation (28, 29). In *B. subtilis*, only few NaOCl-sensitive proteins were identified in the 2D gel-based thiol-redox proteome. One reason for the observed differences in the redox proteome analyses between *E. coli* and *B. subtilis* could be that only abundant cytoplasmic proteins with reversible thiol-modifications are visualized by the 2D gel-based approach (*e.g.* MetE and GapA) and that the gel-free OxICAT approach is much more sensitive for identification of oxidized

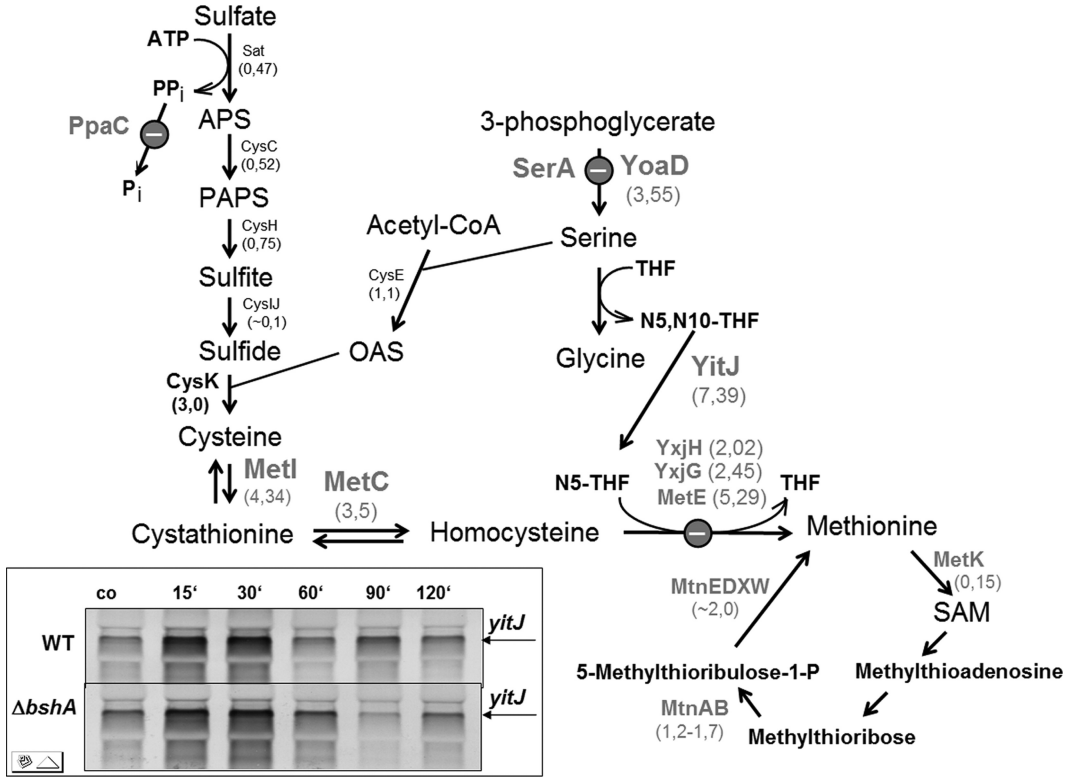


FIG. 7. **Pathways for sulfur assimilation, cysteine and methionine biosynthesis, and induction of S-box regulon genes in response to NaOCl stress.** The S-box regulon gene products that are induced in the transcriptome as a result of methionine starvation provoked by the S-bacillithiolation of MetE and YxjG are bold-faced in gray. The transcriptome induction ratios are shown below the gene products. The gene products of the sulfate assimilation pathway (Sat, CysC, CysH, CysJI, CysE) are not induced upon NaOCl stress (except for CysK). The inset shows the transcriptional induction of *yitJ* in the wild type and Δ*bshA* mutant using Northern blot analysis before (co) and at different times (10, 30, 60, 90, and 120 min) after exposure to 50 $\mu$M NaOCl stress. Abbreviations: APS, adenosine-5′-phosphosulfate; PAPS, 3′-phosphoadenosine-5′-phosphosulfate; OAS, O-acetylserine; N5,N10-THF, 5,10-methylenetetrahydrofolate; N5 -THF, 5-methyltetrahydrofolate; THF, tetrahydrofolate. This figure was adapted from Tomsic *et al.*, 2008 (52).

proteins of lower abundance. However, previous 2Dgel-based redox proteomics analyses in *B. subtilis* have shown that only toxic peroxide concentrations cause increased reversible thiol-oxidations and that only few proteins are oxidized upon paraquat stress (38). Moreover, no reversible thiol-modifications could be monitored using the 2D gel-based approach in response to nitric oxide (NO) in *B. subtilis* (72). In contrast again, several targets for reversible thiol-modifications were identified by NO stress in *E. coli* by the 2D gel-based approach (73). Thus, there might be differences in the extents of reversible thiol-modifiations in response to ROS and RNS between *E. coli* and *B. subtilis.* To address this point, more sensitive gel-free quantifications of reversibly oxidized proteins using the OxICAT approach are required in the future to quantify the changes in the redox proteome of *B. subtilis* more comprehensively. Nevertheless, we show here that NaOCl leads to S-bacillithiolation of selective proteins in *B. subtilis* that play essential roles in protection against hypochloric acid toxicity.

*GapA is Oxidized to an Intramolecular Disulfide Upon NaOCl Stress*—One of the strongest targets that forms intramolecular disulfides upon NaOCl stress was identified as the GapA protein. This confirms previous results in *E. coli* using the OxICAT approach suggesting that GapA is oxidized to an intramolacular disulfide by NaOCl stress (28). GapDH activity was also inactivated by NaOCl in endothelial cells accompanied by thiol depeletion (74). GapA has been shown as redox-controlled cytoplasmic enzyme in prokaryotes and yeast and is susceptible also for inactivation by *S*-sulfenylation, *S*-sulfonylation, *S*-glutathionylation, *S*-nitrosylation, and intermolecular aggregation in response to ROS and RNS (13). GapA is also strongly oxidized by diamide and quinones in *B. subtilis* (21–22). The reversible inactivation of GapA's glycolytic activity in *B. subtilis* by the oxidative mode of quinones has been shown in previous studies (21). Inactivation of GapA leads probably to re-routing of glucose-6-phosphate to the pentose phosphate pathway. The function of the pentose phosphate pathway is to increase NADPH levels and provide reducing equivalents for the thioredoxin/thioredoxin reductase system to restore the redox balance of the cell (13).

*S-bacillithiolation Protects Metabolic Enzymes Against Irreversible Overoxidation*—We further demonstrate that six cytoplasmic proteins undergo reversible *S*-bacillithiolations by NaOCl treatment. Protein *S*-thiolation is an important post-

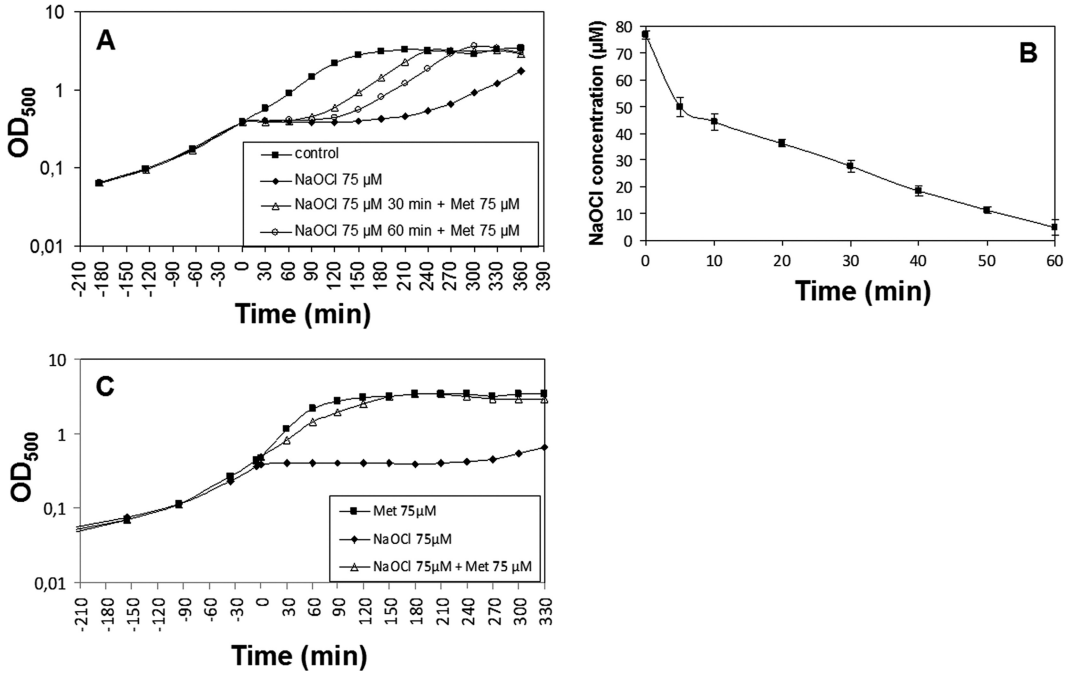


FIG. 8. **NaOCl stress causes methionine auxotrophy that is abolished by methionine addition.** Growth phenotypes of the *B. subtilis* wild type treated with 75 $\mu$M NaOCl at an $OD_{500}$ of 0.4. *A*, Methionine was added 30 or 60 min after exposure to 75 $\mu$M NaOCl stress and the growth was resumed. *B*, The concentrations of consumed NaOCl of wild-type cells were monitored in the culture supernatants after exposure to 75 $\mu$M NaOCl using the FOX assay. The NaOCl concentrations are given as mean values of three independent experiments with error bars. *C*, Methionine (75 $\mu$M) was added after inoculation to the culture at an $OD_{500}$ of 0,07 and 75 $\mu$M NaOCl was added when cells had reached an $OD_{500}$ of 0.4.

translational thiol-modification that occurs in response to oxidative stress in eukaryotic and prokaryotic cells and controls metabolic processes and redox-sensing transcription factors to counteract the cellular damage. In eukaryotes, *S*-glutathionylation is implicated in disease mechanisms, including cell-signaling pathways associated with viral infections and with tumor necrosis factor $\alpha$-induced apoptosis (75). In *E. coli* the activity of the oxidative stress responsive regulator OxyR is controlled by reversible *S*-glutathionylation *in vitro* (11). Moreover, the activities of several metabolic enzymes, such as glyceraldehyde-3-phosphate dehydrogenase, methionine synthase, and the PAPS reductase are inhibited by *S*-glutathionylation in *E. coli* (13, 70, 76). Protein S-thiolation is thought to protect active site Cys residues of essential enzymes against irreversible overoxidation to sulfonic acids. Hypochloric acid shows very fast reaction rates with Cys residues ($K_2 = 3 \times 10^7$ $M^{-1}s^{-1}$) that are seven orders of magnitude higher than measured for peroxides and rapidly lead to irreversible oxidation products, such as sulfinic and sulfonic acids (3, 4, 77, 78). Thus, *S*-bacillithiolation in *B. subtilis* serves to protect active site Cys residues of key metabolic enzymes against irreversible overoxidation by the strong oxidant hypochloric acid.

*The OhrA Peroxiredoxin and the BSH Redox Buffer Confer Protection Against NaOCl*—In *B. subtilis* the OhrR repressor is inactivated by *S*-bacillithiolation after CHP challenge (19). Here we found that *S*-bacillithiolation in response to NaOCl controls OhrR activity resulting in expression of the OhrA peroxiredoxin as protection mechanism (Fig. 9). This expands to role of the thiol-dependent OhrA-like peroxiredoxins in detoxification of hypochloric acid. OhrA-like peroxiredoxins catalyze the reduction of ROOH to their corresponding alcohols (79). The structure of the *Pseudomonas* Ohr peroxiredoxin has been resolved, which is a homodimer consisting of a tightly folded $\alpha/\beta$ fold with two active site cysteines located at the monomer interface on opposite sites of the molecule (80, 81). The mechanism of hydroperoxide reduction is similar to the structurally unrelated eukaryotic 2-Cys peroxiredoxins that exhibit very high specificity and reaction rates with peroxides (81). The catalytic mechanism of peroxiredoxins involves the attack of the hyproperoxide substrate by the active site Cys thiolate (the peroxidatic Cys) that is oxidized to a sulfenic acid intermediate with the release of the alcohol. The peroxiredoxin sulfenic acid undergoes intersubunit or intramolecular disulfide bond formation with the resolving Cys located in the same or another subunit of the dimer. The enzyme is regenerated by thiol-disulfide exchange with GSH or protein electron donors (82). Our results show that OhrA confers specific protection against NaOCl. This leads to the question by which mechanism OhrA is able to detoxify hypochloric acid?

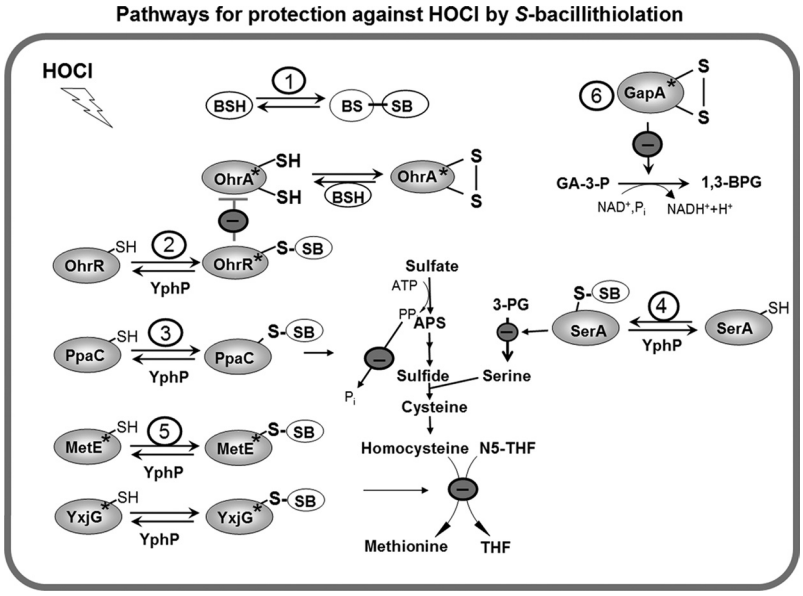


FIG. 9. **Proposed defensive mechanisms against hypochloric acid stress in *B. subtilis.*** Exposure of *B. subtilis* to NaOCl induces an oxidative, disulfide and general stress response (OhrR, Spx, CtsR, PerR, SigmaB). NaOCl leads to *S*-bacillithiolation of OhrR, MetE, YxjG, PpaC, SerA, and YphP and to intramolecular disulfide formation in GapA. The thiol-disulfide isomerase YphP could function as bacilliredoxin in reduction of S-bacillithiolated proteins. (1) The redox buffer BSH could be directly involved in NaOCl detoxification leading to BSSB formation. (2) *S*-bacillithiolation of OhrR causes induction of the OhrA peroxiredoxin that is involved in specific NaOCl detoxification. (3) *S*-bacillithiolation of the inorganic pyrophosphatase PpaC could lead to decreased ATP sulfurylase activity as the removal of $PP_i$ is prevented. (4) S-bacillithiolation of the phosphoglycerate dehydrogenase SerA causes decreased levels of serine that is required for cysteine and methionine biosynthesis. (5) *S*-bacillithiolation of the active site Cys residues of MetE and YxjG leads to methionine auxotrophy to stop translation during the time of NaOCl detoxification (6) The glyceraldehyde-3-phosphate dehydrogenase GapA is inhibited causing decreased glycolysis. The stars indicate the redox-sensing Cys residues that are S-bacillithiolated in OhrR (Cys15), MetE (Cys730), YxjG (Cys346), or oxidized to an intramolecular disulfide in GapA (Cys152). Abbreviations: APS, adenosine-5′-phosphosulfate; N5-THF, 5-methyltetrahydrofolate; THF, tetrahydrofolate; 3-PG, 3-D-phosphoglycerate, GA-3-P, glyceraldehyde-3-phosphate; 1,3-BPG, 1,3-Bisphosphoglycerate.

The reaction of hypochloric acid with Cys proceeds via chlorination of the thiol group to form the unstable sulfenylchloride intermediate that reacts with another thiol group to form a disulfide (3, 4). It could be possible that the OhrA peroxiredoxin is attacked at the peroxidatic Cys by chlorination, resulting in OhrA sulfenylchloride formation and further oxidation to the OhrA inter/intrasubunit disulfide between peroxidatic and resolving Cys residues (Fig. 9). The OhrA disulfide could be regenerated by the BSH redox buffer.

In addition, BSH likely plays a direct role in detoxification of hypochloric acid as has been shown in *E. coli* for GSH (69). The reaction of GSH with hypochloric acid is spontaneous and does not involve conjugating enzymes such as glutathione *S*-transferases (GSTs) (83). GSH is oxidized to GSSG by hypochloric acid nonenzymatically very efficiently as 1 Mol GSH reacted with 4 Mol hypochloric acid *in vitro*. Hypochloric acid likely also oxidizes BSH directly to BSSB in *B. subtilis*.

*Four Enzymes of the Methionine Synthesis Pathway (MetE, YxjG, PpaC, SerA) are S-Bacillithiolated by NaOCl Stress Leading to Methionine Auxotrophy*—Besides OhrR, we identified four enzymes with S-bacillithiolations in response to NaOCl stress as MetE, YxjG, PpaC, and SerA. The methionine synthase MetE has two Zn-coordinating active-site Cys residues in positions 647 and 730 that align with Cys643 and Cys726 of *E. coli* MetE and with Cys620 and Cys704 of *Thermotoga maritima* MetE (84, 85). MetE is *S*-bacillithiolated at the non-essential Cys719 and the Zn-binding ligand Cys730 and the methionine synthase paralog YxjG is S-bacillithiolated at Cys346 that aligns with Cys730 in MetE. In addition, Cys730 of MetE is also S-cysteinylated by NaOCl stress in the wild type as well as in the *bshA* mutant. The *E. coli* MetE protein is *S*-glutathionylated at the nonessential Cys645 in response to diamide that is not conserved in *B. subtilis* MetE (71). In *E. coli* MetE Cys645 is positioned at the entrance of the active Zn site within a cleft between two $\beta_8\alpha_8$ barrels and it's glutathionylation leads to conformational changes of the homocysteine binding active site (70, 85). In *B. subtilis* MetE the non-essential Cys719 is about 20 Å apart from the active site Cys730. This indicates that thiol-disulfide exchange between Cys719 and Cys730 residues is not possible. The question arises how BSH get's access to the active site Zn center in *B. subtilis* MetE ? Recent structural characterizations of the *T. maritima* MetE Zn center in the substrate-free and homocysteine-bound states have revealed an elastic nature of the catalytic Zn center upon substrate binding (84). Homocysteine binding leads to an unexpected inversion of Zn geometry with displacement of the endogenous Zn ligand Glu642 of MetE and movement of the Zn relative to the protein

scaffold. It is proposed that this Zn geometry inversion enhances the nucleophilic activation of the homocysteine thiolate that is required for methyl transfer (84). The dynamic nature and flexibility of the Zn center could also provide access for oxidation of the Zn ligand Cys730 by BSH.

There are also structural differences between GSH and BSH that could explain why BSH has access to the active site Zn center. GSH consists of the tripeptide L-γ-glutamylcysteinylglycine with the Cys bound N-terminally and C-terminally by glutamate and glycine residues that could preclude the accessability of the Cys thiol to the active site in MetE of *E. coli*. The structure of BSH was determined as N-cysteinyl-α-D-glucosaminyl L-malate (20) with an N-terminally located Cys that enables access of the thiol to the active site Zn center of MetE.

Our transcriptional data and growth assays support the methionine starvation phenotype of NaOCl-treated cells that is caused by MetE and YxjG inactivation via S-bacillithiolation. The inactivation of MetE by oxidative stress has important consequences for the cell. The initiation of translation requires formyl-Met as start methionine and depletion of methionine is discussed as checkpoint to stop translation (70). The inactivation of MetE by *S*-bacillithiolation could cause inhibition of translation to prevent further protein damage allowing the cell to detoxify the oxidant and to restore the thiol redox homeostasis. Another possibility could be that MetE inactivation serves to increase cysteine levels. This has been discussed in response to diamide stress that leads to MetE inactivation via S-cysteinylation (67). The CymR-controlled cystathionine beta-synthase MccA and cystathionine lyase MccB are involved in the methionine-to cysteine conversion (Mcc) pathway (51, 86). The *mccAB* operon is strongly up-regulated by diamide stress supporting that homocysteine is converted to cysteine via this Mcc pathway. However, the *mccAB* operon was not induced by NaOCl stress, indicating that S-bacillithiolation of MetE leads to methionine starvation, but not to conversion of homocysteine to cysteine.

Besides MetE and YxjG, the pyrophosphatase PpaC and the 3-D-phosphoglycerate dehydrogenase SerA were identified as S-bacillithiolated that also function in the methionine biosynthesis pathway. PpaC is an essential and conserved enzyme that catalyzes the hydrolysis of inorganic pyrophosphate ($PP_i$). Pyrophosphate is generated in a number of ATP-driven cellular processes, including also the ATP sulfurylation as first step of the sulfate assimilation pathway (87, 88). Efficient removal of $PP_i$ is required to drive the forward direction in these reactions. Thus, inhibition of PpaC activity by S-thiolation could further contribute to methionine starvation. SerA is the first enzyme in the L-serine biosynthetic pathway catalyzing the conversion of 3-D-phosphoglycerate to 3-phosphonooxypyruvate with the generation of NADH. Since serine is used as precursor for cysteine biosynthesis, it's inactivation could pronouce the methionine starvation phenotype.

*The S-Bacillithiolated Disulfide Isomerase YphP Could Function as Putative Bacilliredoxin*—The putative disulfide isomerase YphP was identified as novel S-bacillithiolated protein. YphP is a member of the DUF1094 family with a conserved CXC motif and a thioredoxin-like structure (68). It has been shown that YphP functions as thiol-disulfide isomerase *in vitro*, but the specific substrate is unknown. Phylogenetical studies suggest that YphP could be a novel bacilliredoxin that co-occurs with the enzymes of the BSH biosynthesis pathway across different genomes of low GC Gram-positive bacteria (35). Because YphP is S-bacillithiolated at the active site Cys53, it is likely that YphP might function in de-bacillithiolation of MetE, YxjG, PpaC and SerA upon return to nonstress conditions *in vivo*. Thus, our proteome-wide studies have discovered physiological substrates of the methionine biosynthesis pathway as targets for S-bacillithiolation by NaOCl and a candidate bacilliredoxin that might catalyze the reduction of these protein mixed disulfides.

*Why Causes NaOCl S-Bacillithiolation and Diamide S-Cysteinylation in the Proteome?*—Previous proteome analyses revealed that diamide causes *S*-cysteinylation in six cytoplasmic proteins but no S-bacillithiolations (67). Three of these *S*-cysteinylated proteins (MetE, PpaC and SerA) were identified as *S*-bacillithiolated by NaOCl. This raises the question why S-bacillithiolation was not observed by diamide stress? The answer could be the different thiol chemistries of diamide and NaOCl. Diamide is an electrophilic azocompound that does not oxidize redox-sensitive Cys residues to reactive sulfenic acids or sulfenylchloride. This is supported by the fact that diamide stress does not lead to inactivation of the OhrR repressor (Fig. 3), which would require oxidation of the Cys15 thiolate which then undergoes *S*-bacillithiolation. Instead, diamide forms directly disulfide bonds between two Cys-thiols via an Michael addition reaction of the electrophilic azogroup with two nucleophilic Cys thiol groups (89). Thus, *S*-bacillithiolation requires probably strong oxidants such as NaOCl that oxidize peroxidatic Cys residues first to reactive sulfenic acids or sulfenylchloride.

Another question is why S-cysteinylation and S-bacillithiolation was observed after NaOCl stress ? The observed *S*-cysteinylations could originate from *S*-bacillithiolations that could be explained by the BSH biosynthesis pathway. The pathways for BSH biosynthesis and degradation have been identified in *B. subtilis* and the structures of the L-malic acid glycosyltransferase BaBshA and the GlcNAc-Mal deacetylase BaBshB have been resolved in *B. anthracis* (35, 90). There are two GlcNAc-Mal deacetylases in *B. subtilis*, BshB1 and BshB2 with similar activities. It is postulated that one of these deacetylases could function as bacillithiol-*S*-conjugate amidase (likewise to the Mca mycothiol-*S*-conjugate amidase in Mycobacteria) to cleave conjugates formed by reaction of electrophiles with BSH (35, 91, 92). In turn, BshB1 and/or BshB2 could also cleave GlcN-Mal from *S*-bacillithiolated proteins leaving *S*-cysteinylated proteins. Thus, *S*-cysteinylated proteins observed after NaOCl stress could originate from *S*-bacillithiolations that are cleaved by BshB *in vivo* (91).

The CID MS/MS spectra of the S-bacillithiolated peptides also point to a fragmentation of BSH itself because characteristical fragment and precursor ions appeared that have lost malate. Thus, it is possible that further loss of GlcN in the collision cell leads to "artificial" S-cysteinylated peptides as a result of fragmentation. However, the redox buffer cysteine can be also directly used for S-cysteinylations as shown by identification of S-cysteinylated MetE in the Δ*bshA* mutant. Thus, cysteine can replace BSH for S-thiolation of MetE and OhrR (19, 35). Future proteomic approaches will be directed to quantify the levels of *S*-cysteinylations and *S*-bacillithiolations in the proteome.

In conclusion, we show here that *S*-bacillithiolation is a regulatory redox-switch that occurs in response to hypochloric acid, that is produced in activated macrophages as part of the host immune defense. Thus, Gram-positive pathogens, such as *S. aureus* could use BSH as weapon against the host immune system. OhrA-like peroxiredoxins are controlled by the one-Cys OhrR-family repressors SarZ and MgrA in *S. aureus*, that are inactivated by *S*-thiolation mechanisms *in vitro* (18, 93). Furthermore, reversible thiol-modifications are also widespread in the redox proteome of *S. aureus* by diamide stress including a MetE homolog (22, 94). Thus, our studies provide important leads to future studies on Gram-positive pathogens to study the impact of *S*-bacillithiolations in redox-regulation of OhrR and MetE homologs as defense mechanisms against the host immune system.

*Acknowledgments*—We thank the Decodon company for support with the Decodon Delta 2D software, Dirk Albrecht for the MALDI-TOF analysis, Dana Clausen and Anja Wiechert for excellent technical assistance. We further thank two anonymous reviewers for valuable comments and suggestions to improve this manuscript. We are especially thankful for the advise of one reviewer that the precursor and y ions in the MS/MS spectra of the bacillithiolated peptides have lost malate. We further thank the PRIDE team for support in processing and submission of the LC-MS/MS results to the PRIDE database. We are very grateful to Ahmed Gaballa and John D. Helmann for discussion of the results prior to publication and for providing the *B. subtilis ohrR*-FLAG strain (HB9121), the *ohrR*C15S mutant strain (HB2048) and the *bshA* und *bshB1B2* mutants (HB11002 and HB11053). We further thank Kazuo Kobayashi for the Δ*ohrR*, Δ*sigB* and Δ*perR* mutants and Peter Zuber for the Δ*spx* mutant. We are grateful to Gottfried Palm for stimulating discussions about our model of hypochloric acid chemistry and the structure of the MetE active site.

* This work was supported by a grant from the Deutsche Forschungsgemeinschaft (AN 746/2-1) to H. A.

Ⓢ This article contains supplemental Tables S1 to S4 and Figs. S1 to S5.

¶ To whom correspondence should be addressed: Institute for Microbiology, Ernst-Moritz-Arndt-University of Greifswald, D-17487 Greifswald, Germany. Tel.: +49-3834-864237; Fax: +49-3834-864202; E-mail: antelman@uni-greifswald.de.

REFERENCES

1. Imlay, J. A. (2003) Pathways of oxidative damage. *Annu. Rev. Microbiol.* **57,** 395–418
2. Imlay, J. A. (2008) Cellular defenses against superoxide and hydrogen peroxide. *Annu. Rev. Biochem.* **77,** 755–776
3. Davies, M. J. (2011) Myeloperoxidase-derived oxidation: mechanisms of biological damage and its prevention. *J. Clin. Biochem. Nutr.* **48,** 8–19
4. Hawkins, C. L., Pattison, D. I., and Davies, M. J. (2003) Hypochlorite-induced oxidation of amino acids, peptides and proteins. *Amino Acids* **25,** 259–274
5. Faulkner, M. J., and Helmann, J. D. (2011) Peroxide stress elicits adaptive changes in bacterial metal ion homeostasis. *Antioxid Redox Signal.* doi 10.1089/ars.2010.3682
6. Mongkolsuk, S., and Helmann, J. D. (2002) Regulation of inducible peroxide stress responses. *Mol. Microbiol.* **45,** 9–15
7. Antelmann, H., and Helmann, J. D. (2011) Thiol-based Redox Switches and Gene Regulation. *Antioxid Redox Signal.* **14,** 1049–1063
8. Zheng, M., Aslund, F., and Storz, G. (1998) Activation of the OxyR transcription factor by reversible disulfide bond formation. *Science* **279,** 1718–1721
9. Lee, C., Lee, S. M., Mukhopadhyay, P., Kim, S. J., Lee, S. C., Ahn, W. S., Yu, M. H., Storz, G., and Ryu, S. E. (2004) Redox regulation of OxyR requires specific disulfide bond formation involving a rapid kinetic reaction path. *Nat. Struct. Mol. Biol.* **11,** 1179–1185
10. Choi, H., Kim, S., Mukhopadhyay, P., Cho, S., Woo, J., Storz, G., and Ryu, S. E. (2001) Structural basis of the redox switch in the OxyR transcription factor. *Cell* **105,** 103–113
11. Kim, S. O., Merchant, K., Nudelman, R., Beyer, W. F., Jr., Keng, T., DeAngelo, J., Hausladen, A., and Stamler, J. S. (2002) OxyR: a molecular code for redox-related signaling. *Cell* **109,** 383–396
12. D'Autréaux, B., and Toledano, M. B. (2007) ROS as signalling molecules: mechanisms that generate specificity in ROS homeostasis. *Nat. Rev. Mol. Cell Biol.* **8,** 813–824
13. Brandes, N., Schmitt, S., and Jakob, U. (2009) Thiol-based redox switches in eukaryotic proteins. *Antioxid Redox Signal* **11,** 997–1014
14. Lee, J. W., and Helmann, J. D. (2006) The PerR transcription factor senses H2O2 by metal-catalysed histidine oxidation. *Nature* **440,** 363–367
15. Traoré, D. A., El Ghazouani, A., Jacquamet, L., Borel, F., Ferrer, J. L., Lascoux, D., Ravanat, J. L., Jaquinod, M., Blondin, G., Caux-Thang, C., Duarte, V., and Latour, J. M. (2009) Structural and functional characterization of 2-oxo-histidine in oxidized PerR protein. *Nat. Chem. Biol.* **5,** 53–59
16. Jacquamet, L., Traoré, D. A., Ferrer, J. L., Proux, O., Testemale, D., Hazemann, J. L., Nazarenko, E., El Ghazouani, A., Caux-Thang, C., Duarte, V., and Latour, J. M. (2009) Structural characterization of the active form of PerR: insights into the metal-induced activation of PerR and Fur proteins for DNA binding. *Mol. Microbiol.* **73,** 20–31
17. Panmanee, W., Vattanaviboon, P., Poole, L. B., and Mongkolsuk, S. (2006) Novel organic hydroperoxide-sensing and responding mechanisms for OhrR, a major bacterial sensor and regulator of organic hydroperoxide stress. *J. Bacteriol.* **188,** 1389–1395
18. Chen, P. R., Brugarolas, P., and He, C. (2011) Redox Signaling in Human Pathogens. *Antioxid Redox Signal.* **14,** 1107–1118
19. Lee, J. W., Soonsanga, S., and Helmann, J. D. (2007) A complex thiolate switch regulates the Bacillus subtilis organic peroxide sensor OhrR. *Proc. Natl. Acad. Sci. U.S.A.* **104,** 8743–8748
20. Newton, G. L., Rawat, M., La Clair, J. J., Jothivasan, V. K., Budiarto, T., Hamilton, C. J., Claiborne, A., Helmann, J. D., and Fahey, R. C. (2009) Bacillithiol is an antioxidant thiol produced in Bacilli. *Nat. Chem. Biol.* **5,** 625–627
21. Liebeke, M., Pöther, D. C., van Duy, N., Albrecht, D., Becher, D., Hochgräfe, F., Lalk, M., Hecker, M., and Antelmann, H. (2008) Depletion of thiol-containing proteins in response to quinones in Bacillus subtilis. *Mol. Microbiol.* **69,** 1513–1529
22. Pöther, D. C., Liebeke, M., Hochgräfe, F., Antelmann, H., Becher, D., Lalk, M., Lindequist, U., Borovok, I., Cohen, G., Aharonowitz, Y., and Hecker, M. (2009) Diamide triggers mainly S Thiolations in the cytoplasmic proteomes of Bacillus subtilis and Staphylococcus aureus. *J. Bacteriol.* **191,** 7520–7530
23. Nguyen, T. T., Eiamphungporn, W., Mäder, U., Liebeke, M., Lalk, M., Hecker, M., Helmann, J. D., and Antelmann, H. (2009) Genome-wide responses to carbonyl electrophiles in Bacillus subtilis: control of the thiol-dependent formaldehyde dehydrogenase AdhA and cysteine proteinase YraA by the MerR-family regulator YraB (AdhR). *Mol. Microbiol.* **71,** 876–894
24. Chi, B. K., Albrecht, D., Gronau, K., Becher, D., Hecker, M., and Antelmann,

H. (2010) The redox-sensing regulator YodB senses quinones and diamide via a thiol-disulfide switch in Bacillus subtilis. *Proteomics* **10,** 3155–3164
25. Chi, B. K., Kobayashi, K., Albrecht, D., Hecker, M., and Antelmann, H. (2010) The paralogous MarR/DUF24-family repressors YodB and CatR control expression of the catechol dioxygenase CatE in Bacillus subtilis. *J. Bacteriol.* **192,** 4571–4581
26. Leelakriangsak, M., Huyen, N. T., Töwe, S., van Duy, N., Becher, D., Hecker, M., Antelmann, H., and Zuber, P. (2008) Regulation of quinone detoxification by the thiol stress sensing DUF24/MarR-like repressor, YodB in Bacillus subtilis. *Mol. Microbiol.* **67,** 1108–1124
27. Touati, D., Jacques, M., Tardat, B., Bouchard, L., and Despied, S. (1995) Lethal oxidative damage and mutagenesis are generated by iron in delta fur mutants of Escherichia coli: protective role of superoxide dismutase. *J. Bacteriol.* **177,** 2305–2314
28. Leichert, L. I., Gehrke, F., Gudiseva, H. V., Blackwell, T., Ilbert, M., Walker, A. K., Strahler, J. R., Andrews, P. C., and Jakob, U. (2008) Quantifying changes in the thiol redox proteome upon oxidative stress in vivo. *Proc. Natl. Acad. Sci. U.S.A.* **105,** 8197–8202
29. Winter, J., Ilbert, M., Graf, P. C., Ozcelik, D., and Jakob, U. (2008) Bleach activates a redox-regulated chaperone by oxidative protein unfolding. *Cell* **135,** 691–701
30. Wang, S., Deng, K., Zaremba, S., Deng, X., Lin, C., Wang, Q., Tortorello, M. L., and Zhang, W. (2009) Transcriptomic response of Escherichia coli O157:H7 to oxidative stress. *Appl. Environ. Microbiol.* **75,** 6110–6123
31. Ceragioli, M., Mols, M., Moezelaar, R., Ghelardi, E., Senesi, S., and Abee, T. (2010) Comparative transcriptomic and phenotypic analysis of the responses of Bacillus cereus to various disinfectant treatments. *Appl. Environ. Microbiol.* **76,** 3352–3360
32. Nakano, M. M., Hajarizadeh, F., Zhu, Y., and Zuber, P. (2001) Loss-of-function mutations in yjbD result in ClpX- and ClpP-independent competence development of Bacillus subtilis. *Mol. Microbiol.* **42,** 383–394
33. Hayashi, K., Kensuke, T., Kobayashi, K., Ogasawara, N., and Ogura, M. (2006) Bacillus subtilis RghR (YvaN) represses rapG and rapH, which encode inhibitors of expression of the srfA operon. *Mol. Microbiol.* **59,** 1714–1729
34. Fuangthong, M., and Helmann, J. D. (2002) The OhrR repressor senses organic hydroperoxides by reversible formation of a cysteine-sulfenic acid derivative. *Proc. Natl. Acad. Sci. U.S.A.* **99,** 6690–6695
35. Gaballa, A., Newton, G. L., Antelmann, H., Parsonage, D., Upton, H., Rawat, M., Claiborne, A., Fahey, R. C., and Helmann, J. D. (2010) Biosynthesis and functions of bacillithiol, a major low-molecular-weight thiol in Bacilli. *Proc. Natl. Acad. Sci. U.S.A.* **107,** 6482–6486
36. Stülke, J., Hanschke, R., and Hecker, M. (1993) Temporal activation of beta-glucanase synthesis in Bacillus subtilis is mediated by the GTP pool. *J. Gen. Microbiol.* **139,** 2041–2045
37. Nourooz-Zadeh, J., Tajaddini-Sarmadi, J., and Wolff, S. P. (1994) Measurement of plasma hydroperoxide concentrations by the ferrous oxidation-xylenol orange assay in conjunction with triphenylphosphine. *Anal. Biochem.* **220,** 403–409
38. Hochgräfe, F., Mostertz, J., Albrecht, D., and Hecker, M. (2005) Fluorescence thiol modification assay: oxidatively modified proteins in Bacillus subtilis. *Mol. Microbiol.* **58,** 409–425
39. Barbe, V., Cruveiller, S., Kunst, F., Lenoble, P., Meurice, G., Sekowska, A., Vallenet, D., Wang, T., Moszer, I., Médigue, C., and Danchin, A. (2009) From a consortium sequence to a unified sequence: the Bacillus subtilis 168 reference genome a decade later. *Microbiology* **155,** 1758–1775
40. Elias, J. E., and Gygi, S. P. (2007) Target-decoy search strategy for increased confidence in large-scale protein identifications by mass spectrometry. *Nat. Methods* **4,** 207–214
41. Vizcaino, J. A., Côté, R., Reisinger, F., Barsnes, H., Foster, J. M., Rameseder, J., Hermjakob, H., and Martens, L. (2010) The Proteomics Identifications database: 2010 update. *Nucleic Acids Res.* **38,** D736–742
42. Majumdar, D., Avissar, Y. J., and Wyche, J. H. (1991) Simultaneous and rapid isolation of bacterial and eukaryotic DNA and RNA: a new approach for isolating DNA. *BioTechniques* **11,** 94–101
43. Charbonnier, Y., Gettler, B., François, P., Bento, M., Renzoni, A., Vaudaux, P., Schlegel, W., and Schrenzel, J. (2005) A generic approach for the design of whole-genome oligoarrays, validated for genomotyping, deletion mapping and gene expression analysis on Staphylococcus aureus. *BMC Genomics* **6,** 95
44. de Hoon, M. J., Imoto, S., Nolan, J., and Miyano, S. (2004) Open source clustering software. *Bioinformatics* **20,** 1453–1454
45. Leichert, L. I., Scharf, C., and Hecker, M. (2003) Global characterization of disulfide stress in Bacillus subtilis. *J. Bacteriol.* **185,** 1967–1975
46. Nguyen, V. D., Wolf, C., Mäder, U., Lalk, M., Langer, P., Lindequist, U., Hecker, M., and Antelmann, H. (2007) Transcriptome and proteome analyses in response to 2-methylhydroquinone and 6-brom-2-vinyl-chroman-4-on reveal different degradation systems involved in the catabolism of aromatic compounds in Bacillus subtilis. *Proteomics* **7,** 1391–1408
47. Tam le, T., Eymann, C., Albrecht, D., Sietmann, R., Schauer, F., Hecker, M., and Antelmann, H. (2006) Differential gene expression in response to phenol and catechol reveals different metabolic activities for the degradation of aromatic compounds in Bacillus subtilis. *Environ. Microbiol.* **8,** 1408–1427
48. Eisen, M. B., Spellman, P. T., Brown, P. O., and Botstein, D. (1998) Cluster analysis and display of genome-wide expression patterns. *Proc. Natl. Acad. Sci. U.S.A.* **95,** 14863–14868
49. Wetzstein, M., Völker, U., Dedio, J., Löbau, S., Zuber, U., Schiesswohl, M., Herget, C., Hecker, M., and Schumann, W. (1992) Cloning, sequencing, and molecular analysis of the dnaK locus from Bacillus subtilis. *J. Bacteriol.* **174,** 3300–3310
50. Antelmann, H., Hecker, M., and Zuber, P. (2008) Proteomic signatures uncover thiol-specific electrophile resistance mechanisms in Bacillus subtilis. *Expert Rev. Proteomics* **5,** 77–90
51. Even, S., Burguière, P., Auger, S., Soutourina, O., Danchin, A., and Martin-Verstraete, I. (2006) Global control of cysteine metabolism by CymR in Bacillus subtilis. *J. Bacteriol.* **188,** 2184–2197
52. Tomsic, J., McDaniel, B. A., Grundy, F. J., and Henkin, T. M. (2008) Natural variability in S-adenosylmethionine (SAM)-dependent riboswitches: S-box elements in bacillus subtilis exhibit differential sensitivity to SAM In vivo and in vitro. *J. Bacteriol.* **190,** 823–833
53. Henkin, T. M. (2008) Riboswitch RNAs: using RNA to sense cellular metabolism. *Genes Dev.* **22,** 3383–3390
54. Henkin, T. M. (2009) RNA-dependent RNA switches in bacteria. *Methods Mol. Biol.* **540,** 207–214
55. Grundy, F. J., and Henkin, T. M. (2003) The T box and S box transcription termination control systems. *Front. Biosci.* **8,** d20–31
56. Szegedi, S. S., Castro, C. C., Koutmos, M., and Garrow, T. A. (2008) Betaine-homocysteine S-methyltransferase-2 is an S-methylmethionine-homocysteine methyltransferase. *J. Biol. Chem.* **283,** 8939–8945
57. Mansilla, M. C., Albanesi, D., and de Mendoza, D. (2000) Transcriptional control of the sulfur-regulated cysH operon, containing genes involved in L-cysteine biosynthesis in Bacillus subtilis. *J. Bacteriol.* **182,** 5885–5892
58. Yurimoto, H., Hirai, R., Matsuno, N., Yasueda, H., Kato, N., and Sakai, Y. (2005) HxlR, a member of the DUF24 protein family, is a DNA-binding protein that acts as a positive regulator of the formaldehyde-inducible hxlAB operon in Bacillus subtilis. *Mol. Microbiol.* **57,** 511–519
59. Moore, C. M., Gaballa, A., Hui, M., Ye, R. W., and Helmann, J. D. (2005) Genetic and physiological responses of Bacillus subtilis to metal ion stress. *Mol. Microbiol.* **57,** 27–40
60. Moore, C. M., and Helmann, J. D. (2005) Metal ion homeostasis in Bacillus subtilis. *Curr. Opin. Microbiol.* **8,** 188–195
61. Smaldone, G. T., and Helmann, J. D. (2007) CsoR regulates the copper efflux operon copZA in Bacillus subtilis. *Microbiology* **153,** 4123–4128
62. Szurmant, H., and Ordal, G. W. (2004) Diversity in chemotaxis mechanisms among the bacteria and archaea. *Microbiol. Mol. Biol. Rev.* **68,** 301–319
63. Kempf, B., and Bremer, E. (1998) Uptake and synthesis of compatible solutes as microbial stress responses to high-osmolality environments. *Arch. Microbiol.* **170,** 319–330
64. Massey, V., Gibson, Q. H., and Veeger, C. (1960) Intermediates in the catalytic action of lipoyl dehydrogenase (diaphorase). *Biochem. J.* **77,** 341–351
65. Zuber, P. (2004) Spx-RNA polymerase interaction and global transcriptional control during oxidative stress. *J. Bacteriol.* **186,** 1911–1918
66. Zuber, P. (2009) Management of oxidative stress in Bacillus. *Annu. Rev. Microbiol.* **63,** 575–597
67. Hochgräfe, F., Mostertz, J., Pöther, D. C., Becher, D., Helmann, J. D., and Hecker, M. (2007) S-cysteinylation is a general mechanism for thiol protection of Bacillus subtilis proteins after oxidative stress. *J. Biol. Chem.* **282,** 25981–25985

68. Derewenda, U., Boczek, T., Gorres, K. L., Yu, M., Hung, L. W., Cooper, D., Joachimiak, A., Raines, R. T., and Derewenda, Z. S. (2009) Structure and function of Bacillus subtilis YphP, a prokaryotic disulfide isomerase with a CXC catalytic motif. *Biochemistry* **48,** 8664–8671
69. Masip, L., Veeravalli, K., and Georgiou, G. (2006) The many faces of glutathione in bacteria. *Antioxid Redox. Signal.* **8,** 753–762
70. Hondorp, E. R., and Matthews, R. G. (2004) Oxidative stress inactivates cobalamin-independent methionine synthase (MetE) in Escherichia coli. *PLoS Biol.* **2,** e336
71. Hondorp, E. R., and Matthews, R. G. (2009) Oxidation of cysteine 645 of cobalamin-independent methionine synthase causes a methionine limitation in Escherichia coli. *J. Bacteriol.* **191,** 3407–3410
72. Hochgräfe, F., Wolf, C., Fuchs, S., Liebeke, M., Lalk, M., Engelmann, S., and Hecker, M. (2008) Nitric oxide stress induces different responses but mediates comparable protein thiol protection in Bacillus subtilis and Staphylococcus aureus. *J. Bacteriol.* **190,** 4997–5008
73. Brandes, N., Rinck, A., Leichert, L. I., and Jakob, U. (2007) Nitrosative stress treatment of E. coli targets distinct set of thiol-containing proteins. *Mol. Microbiol.* **66,** 901–914
74. Pullar, J. M., Winterbourn, C. C., and Vissers, M. C. (1999) Loss of GSH and thiol enzymes in endothelial cells exposed to sublethal concentrations of hypochlorous acid. *Am. J. Physiol.* **277,** H1505–1512
75. Dalle-Donne, I., Rossi, R., Colombo, G., Giustarini, D., and Milzani, A. (2009) Protein S-glutathionylation: a regulatory device from bacteria to humans. *Trends Biochem. Sci* **34,** 85–96
76. Lillig, C. H., Potamitou, A., Schwenn, J. D., Vlamis-Gardikas, A., and Holmgren, A. (2003) Redox regulation of 3′-phosphoadenylylsulfate reductase from Escherichia coli by glutathione and glutaredoxins. *J. Biol. Chem.* **278,** 22325–22330
77. Winterbourn, C. C., and Hampton, M. B. (2008) Thiol chemistry and specificity in redox signaling. *Free Radic. Biol. Med.* **45,** 549–561
78. Pattison, D. I., and Davies, M. J. (2001) Absolute rate constants for the reaction of hypochlorous acid with protein side chains and peptide bonds. *Chem. Res. Toxicol.* **14,** 1453–1464
79. Dubbs, J. M., and Mongkolsuk, S. (2007) Peroxiredoxins in bacterial antioxidant defense. *Subcell. Biochem.* **44,** 143–193
80. Lesniak, J., Barton, W. A., and Nikolov, D. B. (2002) Structural and functional characterization of the Pseudomonas hydroperoxide resistance protein Ohr. *EMBO J.* **21,** 6649–6659
81. Poole, L. B., and Nelson, K. J. (2008) Discovering mechanisms of signaling-mediated cysteine oxidation. *Curr. Opin. Chem. Biol.* **12,** 18–24
82. Barford, D. (2004) The role of cysteine residues as redox-sensitive regulatory switches. *Curr. Opin. Struct. Biol.* **14,** 679–686
83. Chesney, J. A., Eaton, J. W., and Mahoney, J. R., Jr. (1996) Bacterial glutathione: a sacrificial defense against chlorine compounds. *J. Bacteriol.* **178,** 2131–2135
84. Koutmos, M., Pejchal, R., Bomer, T. M., Matthews, R. G., Smith, J. L., and Ludwig, M. L. (2008) Metal active site elasticity linked to activation of homocysteine in methionine synthases. *Proc. Natl. Acad. Sci. U.S.A.* **105,** 3286–3291
85. Pejchal, R., and Ludwig, M. L. (2005) Cobalamin-independent methionine synthase (MetE): a face-to-face double barrel that evolved by gene duplication. *PLoS Biol.* **3,** e31
86. Hullo, M. F., Auger, S., Soutourina, O., Barzu, O., Yvon, M., Danchin, A., and Martin-Verstraete, I. (2007) Conversion of methionine to cysteine in Bacillus subtilis and its regulation. *J. Bacteriol.* **189,** 187–197
87. Cooperman, B. S., Baykov, A. A., and Lahti, R. (1992) Evolutionary conservation of the active site of soluble inorganic pyrophosphatase. *Trends Biochem. Sci.* **17,** 262–266
88. Lee, H. S., Kim, Y. J., Lee, J. H., and Kang, S. G. (2009) Identification and characterization of inorganic pyrophosphatase and PAP phosphatase from Thermococcus onnurineus NA1. *J. Bacteriol.* **191,** 3415–3419
89. Kosower, N. S., and Kosower, E. M. (1995) Diamide: an oxidant probe for thiols. *Methods Enzymol.* **251,** 123–133
90. Parsonage, D., Newton, G. L., Holder, R. C., Wallace, B. D., Paige, C., Hamilton, C. J., Dos Santos, P. C., Redinbo, M. R., Reid, S. D., and Claiborne, A. (2010) Characterization of the N-acetyl-alpha-D-glucosaminyl l-malate synthase and deacetylase functions for bacillithiol biosynthesis in Bacillus anthracis. *Biochemistry* **49,** 8398–8414
91. Helmann, J. D. (2011) Bacillithiol, a New Player in Bacterial Redox Homeostasis. *Antioxid. Redox. Signal* **15,** 123–133
92. Newton, G. L., Buchmeier, N., and Fahey, R. C. (2008) Biosynthesis and functions of mycothiol, the unique protective thiol of Actinobacteria. *Microbiol. Mol. Biol. Rev.* **72,** 471–494
93. Poor, C. B., Chen, P. R., Duguid, E., Rice, P. A., and He, C. (2009) Crystal structures of the reduced, sulfenic acid, and mixed disulfide forms of SarZ, a redox active global regulator in Staphylococcus aureus. *J. Biol. Chem.* **284,** 23517–23524
94. Wolf, C., Hochgräfe, F., Kusch, H., Albrecht, D., Hecker, M., and Engelmann, S. (2008) Proteomic analysis of antioxidant strategies of Staphylococcus aureus: diverse responses to different oxidants. *Proteomics* **8,** 3139–3153